STRUCTURAL PERFORMANCE OF BAMBOO:

CAPACITY UNDER SUSTAINED LOADS AND MONOTONIC BENDING

by

Jennifer M. Gottron

Bachelor of Science, Kent State University, 2011

Submitted to the Graduate Faculty of

The Swanson School of Engineering in partial fulfillment

of the requirements for the degree of

Master of Science

University of Pittsburgh

2014

UNIVERSITY OF PITTSBURGH

SWANSON SCHOOL OF ENGINEERING

This thesis was presented

by

Jennifer M. Gottron

It was defended on

December 17, 2013

and approved by

Melissa Bilec, Ph.D., Assistant Professor

Department of Civil and Environmental Engineering

John Brigham, Ph.D., Assistant Professor

Department of Civil and Environmental Engineering

Thesis Advisor: Kent A. Harries, Ph.D., Associate Professor

Department of Civil and Environmental Engineering

University of Pittsburgh

STRUCTURAL PERFORMANCE OF BAMBOO:

CAPACITY UNDER SUSTAINED LOADS AND MONOTONIC BENDING

Jennifer M. Gottron, M.S.

University of Pittsburgh, 2014

The exploration of the structural material properties of bamboo is motivated by its potential to serve as an alternative sustainable building material. Although bamboo has been used as a building material for thousands of years, the majority of applications do not conform to any standard design criteria and are therefore considered to be non-, or at best marginally-engineered construction. Nonetheless, as a result of the composite-like structure of bamboo, its mechanical properties are generally superior to those of other natural materials such as timber. The current research addresses the capacity of bamboo under sustained loads and monotonic bending. The sustained loads intend to develop an understanding of the material creep behavior. The effects of creep on radially-cut clear bamboo specimens will be evaluated based on a series of parameters, mainly the ratio of the ultimate load applied to specimen and the orientation of the specimen with respect to the fiber gradation. Specimens were subject to sustained loads for a period of 90 days. Following 10 days of recovery, the residual capacity of the creep specimens was determined. Significant creep-induced plastic deformations and strains were observed in the present work. The orientation of the specimen was found to have a significant effect on both the creep behavior and residual strength of creep-conditioned specimens. The results showed that bamboo loaded

with the outer culm-wall in tension (OT) generally exhibited a greater modulus of rupture but reduced apparent modulus of elasticity and residual strength when compared to specimens with outer culm-wall in compression (OC). Additionally the effects of creep conditioning appear to have a strengthening effect on the residual capacity of OC specimens and a detrimental effects on OT specimens. The results of the creep experiments met or exceeded the ASTM 6815 acceptance criteria for wood suggesting that for the structural design of bamboo, a load duration factor similar to that used for wood may be employed.

While the creep tests explored only one species of bamboo, the culm bending tests investigated the longitudinal shear capacity of two species. Longitudinal splitting often dominates failure in bamboo components; longitudinal splitting in bamboo is thought to be the result of a mixed-mode shear failure which is influenced by both Mode I tension and Mode II shear failures. The research aimed to understand the mixed-mode shear capacity of full-culm bamboo under four point bending by testing standard span culms with longitudinal notches at midspan and unnotched short span culms. Each of the culm bending tests is designed to provoke a mixed-mode shear failure. The data demonstrated a reduction in the pure Mode II capacity of culms in the presence of Mode I component of distortion. Each of the experiments reported maintains the ultimate goal of standardization; the data collected and results provided intend to aid in the development of a standardized design criteria for bamboo structures.

TABLE OF CONTENTS

LIST OF TABLES

LIST OF FIGURES

NOMENCLATURE

2a	initial crack length for split-pin test
a	shear span (creep test)
A	area
b	width
D	outer diameter of culm
D_i	deflection one minute after loading
D_{30}	deflection at 30 days of sustained load
D_{60}	deflection at 60 days of sustained load
D_{90}	deflection at 90 days of sustained load
dv	lever arm of internal force couple
E	modulus of elasticity
F	force (culm bending test)
f_b	average MOR for portion of specimen below neutral axis (creep test)
f_r	average modulus of rupture (creep test)
f_t	average MOR for portion of specimen above neutral axis (creep test)
FD_{90}	90 day fractional deflection
G_I	Mode I strain energy release rate
I	moment of inertia

K_I	crack intensity factor
L	length
M	applied moment
P	applied load (creep test)
P_{ult}	ultimate applied load (creep test)
Q	first moment of area
RC	relative creep
S	clear span from support to support (culm bending test)
t	average culm wall thickness (height of radially cut clear specimens)
y	centroidal axis of clear specimen
y_b	distance from bottom of specimen to shifted neutral axis
y_t	distance from shifted neutral axis to top of specimen
V	shear force
α	neutral axis location as a ratio of specimen height
Δ	initial elastic deflection at midspan
$\varepsilon(t)$	average strain at midspan at time, t
ε_0	average initial strain at midspan
ε_L	average longitudinal strain
ε_T	average tangential strain
ψ_t	creep factor
$\sigma_\perp$	tensile strength perpendicular to bamboo fibers
σ_I	Mode I stress
σ_{ICR}	critical Mode I stress

σ_{II}	Mode II stress
σ_{IICR}	critical Mode II stress

ACKNOWLEDGEMENTS

I would like to thank Dr. Kent Harries for his unwavering guidance and support in the undertaking of the current research. The opportunity to work with and learn from an experienced mentor was sincerely inspiring. Additionally, the research could not have been completed without the help of many others that I would like to acknowledge:

Charles “Scooter” Hager, CEE lab technician, for bringing all ideas to life with his expertise in the structural engineering laboratory.

Committee members, Dr. Melissa Bilec and Dr. John Brigham, for their time, dedication and input in the development of the research.

Dr. Mike Richard for his tremendous guidance and assistance in the development of an interest in bamboo structures and research in general.

Dr. Bhavna Sharma and Dr. Qingfeng Xu for sharing their knowledge of bamboo and for the research that they have contributed to the field.

The 2013 IRES students, Logan Platt, and Dr. Harries’ research group for their much appreciated assistance in the lab.

Watkins-Haggart Structural Engineering Lab for providing the tools to complete the research.

Family and friends for their absolute support and encouragement throughout the entire process.

1.0 INTRODUCTION AND LITERATURE REVIEW

The exploration of the structural material properties of bamboo is motivated by its potential to serve as an alternative sustainable building material. Although bamboo has been used as a building material for thousands of years, the majority of applications do not abide by any standard design criteria. In this context, bamboo construction is considered to be non-, or at best marginally-engineered construction. The lack of standardization is partially due to the economic and technical environment of the regions where bamboo is naturally abundant. The desire to develop standardization for bamboo as a building material is inspired by its generally excellent material characteristics. As a result of the composite-like structure of the bamboo, its mechanical properties are generally superior to those of other natural materials such as timber. Bamboo's availability and relatively rapid growth rate also make it a rapidly renewable resource. In addition to its renewability, the manufacturing process requires less energy and produces less waste than conventional building materials such as steel and concrete. Sharma (2013) introduces the obstacle of the association of bamboo with lower social classes. In developing countries bamboo is considered a "poor-man's material" while conventional building materials such as concrete establish a higher social status. Interestingly, the stigma against bamboo construction may be partially mitigated by "engineering acceptance," that is, standardization.

1.1 COMPOSITION OF BAMBOO

The geometry of bamboo presents an additional interest in the studies of its mechanical properties. The culm is often tapered, and many geometrical characteristics change over the height of the culm. Typically, both the thickness of the wall and the outer diameter decrease as one moves from the bottom to the top of an individual culm. Additionally, the length of the internode often increases with height (Fig 1.1a). This geometry results from the necessity that the top of the culm must remain more flexible than the bottom in its natural environment. The difference in flexibility allows for the bamboo to resist natural forces, such as wind, while maintaining the ability to support itself over very tall heights. The position along the culm also affects the material properties for these reasons.

In addition to the geometry of bamboo, the smaller-scale composition (i.e. fiber volume ratio and density) of bamboo also affects the performance of the material. The fibers within the bamboo are a vital factor when considering the capabilities of the material as a structural member. The fiber density in the cross section of a culm increases towards its outer edges (Fig 1.1b). The gradation of the fibers occurs naturally due to the growth pattern of bamboo. As in engineered composites, the fibers are much stronger than the matrix, and rarely govern failure. The highly isotropic nature of the fibers makes bamboo susceptible to orientation of loading (Janssen 1981). More specifically, the material is much weaker in its transverse direction, restricting its structural capabilities and applications to a certain degree.

Another geometric factor affecting structural applications of bamboo is the straightness of the culm (Fig 1.1c). The severity of the out-of-straightness of bamboo culms may affect their

mechanical properties in addition to their structural performance. Although it has not been thoroughly studied, it is also known that the nodes affect the performance of bamboo. The majority of the culm is made up of internode sections in which the fibers are primarily unidirectional: parallel to the culm. However, because the primarily unidirectional fibers change direction at the node, the node may enhance, impair or simply maintain the specimen's ability to carry a load, depending on the type of load applied. For example, Arce-Villalobos (1993) found the tensile strength at the node to be 80% of the tensile strength at the internode. However, tests suggest that the existence of a node has little effect on the specimen's compressive strength (Janssen 1981; Limaye 1952; Sekhar and Rawat 1956). Janssen (1981) and Mitch (2009) each performed experiments indicating shear strength to have increased values in nodal regions. Similar to the culm's changing geometry and microstructure, the straightness and location of nodes must also be considered in the analysis of material properties. Each of the compositional elements considered may have effects on the overall performance of the culm depending on species. Richard (2013) provides a thorough discussion of the nature and composition of bamboo.

1.2 STANDARDIZATION OF BAMBOO

The International Organization for Standardization (ISO) developed a series of documents to provide standards for bamboo material tests (ISO 2004a) and a model code for design (ISO 2004b). The guidelines within the material test standard address the process of determining only certain physical (percentage of fibers, weight by volume, moisture content, position along the

culm, existence and number of nodes, form of specimen and size of specimen) and mechanical properties including compression, bending, interlaminar shear and tension.

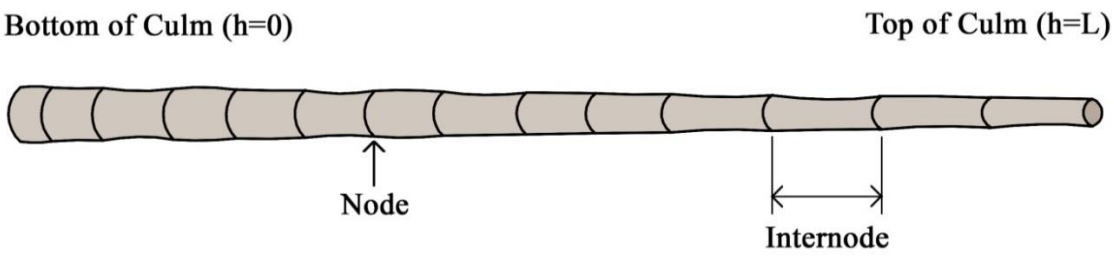

a) typical tapering of culm.

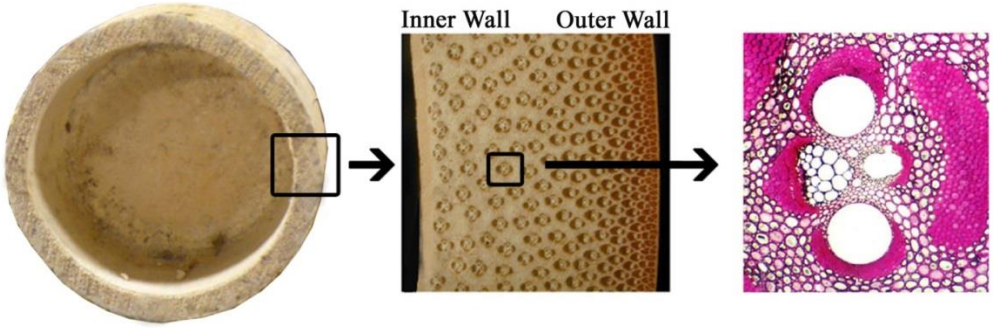

b) typical fiber gradation within culm section.

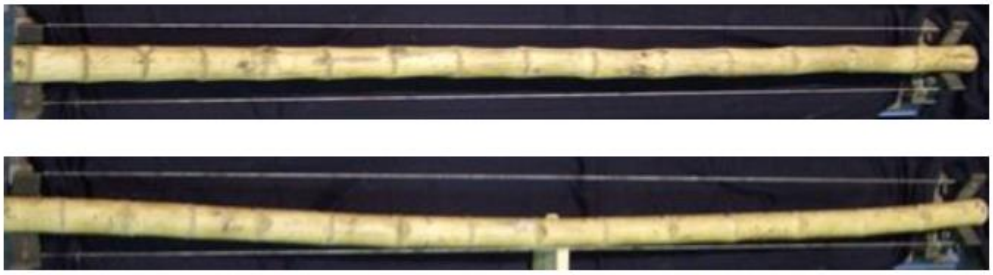

c) variation in straightness of Tre Gai culms of identical "batch" and storage conditions (Richard 2013).

Figure 1. 1: General composition of bamboo.

Although standardization of bamboo is essential to the adoption and development of the material as an engineered building material, many challenges remain. One major burden in the standardization process is the difference in mechanical properties from species to species. The fact that physical characteristics vary between species leads to difficulty in establishing empirical values or relationships. Also contributing to the variation in mechanical properties is the effect of geometric variation and culm orientation relative to applied loads. Orientation of both full-culm and partial-culm specimens are affected by the composition of the fibers. In full-culm tests, the direction of the fibers in relation to the load will generate very different results. For example, compressive and tensile strengths of bamboo are more than an order of magnitude greater when applied parallel to the fibers as opposed to in a transverse manner (Mitch 2010). On a smaller scale, specimens that have been cut from a portion of the culm wall mask the effects of the fiber gradation (Richard 2013). Although advantageous in certain circumstances, the inconsistency of material properties through the wall thickness develops another variable to be considered in material characterization, design and eventual standardization (Fig 1.1b).

Many studies have acknowledged individual variables contributing to the strength of bamboo. More specifically, many of the geometric variables discussed in section 1.1 have been thoroughly analyzed by researchers. Experiments have suggested that the top of a culm (younger material) has better mechanical properties than the bottom of a culm (Ahmad and Kamke 2005). The elastic modulus, flexural strength, impact strength and fracture toughness decrease with culm age at harvest (Low et al. 2006). Flexural deformability is affected by the density of fibers in tension. Fiber density near the outer wall of the bamboo culm is greater than the fiber density at the inner wall of the culm. Whether the outer fiber density of the culm is in compression or tension does not impact the stiffness of the specimen (Obataya et al. 2007). Many additional

experiments have addressed similar issues. The amount of research required in order to generalize the effect of a certain geometric or compositional element on the strength of the bamboo is significant. Therefore, just as any now-conventional building material once did, the standardization of bamboo requires the commitment and collaboration of many researchers.

Aside from the composition-related obstacles, the lack of resources often limits the opportunity to standardize bamboo. One major (and often over-looked) factor associated with the standardization of bamboo is the necessity of practicality. Many of the countries most inclined to utilize bamboo in structures do not have wide-spread access to the equipment or expertise necessary to perform standard material characterization experiments. This additional consideration has inspired the idea of field applicable tests in a portion of the bamboo studies being conducted. Limited availability of resources leads eventually to a lack of communication and the use of ad hoc test procedures which fail to benefit not only those already using bamboo for building but also the advancement of bamboo as an alternative building material. Upon the collaboration of experimental results, the idea of standardization becomes realistic.

1.3 MATERIAL CREEP BEHAVIOR

The phenomenon of creep, particularly in anisotropic and fiber-reinforced materials, is critical to structural design. Creep is defined as the inelastic deformation of a material due to changes in the material caused by the prolonged application of stress (Allen and Iano 2009). Creep effects, at a minimum, have the potential to affect the serviceability of structure. A more severe issue related to creep is its ability to alter material characteristics and subsequent mechanical properties of a structural element or system. Eventually, excessive creep may result in the failure of a structure.

This is often referred to as ‘creep rupture,’ in which a structure fails under the effects of sustained stress which fall below the elastic limit of the material.

Creep may continue until fracture occurs. Alternatively, the rate of creep deformation may decrease and approach zero. The characteristics of creep depend on the material and the conditions under which it is loaded. The strain that results from creep is considered plastic strain. Additionally, if the stress in the member exceeds the elastic limit, permanent deformation occurs and the strain in this case is also considered plastic. When load is applied, the total strain is made up of elastic strain and plastic strain. When the specimen is unloaded, the plastic strain remains while the elastic strain is recovered and returns to zero. For this reason, the strain associated with creep alone is important when considering the lifespan and performance of a structural member (Riley et al. 2002).

Although the creep of bamboo has been considered briefly in previous research (Kanzawa 2011; Jannsen 1981), it often exists only as a supplemental experiment to some primary study. Creep has rarely been the focus of a study, and therefore the available information on the creep of bamboo lacks detail and often useful data. Extensive knowledge in all areas of structural design is vital in the presentation of bamboo as an alternative building material. The goal of the present experimental study is to develop an understanding of the capacity of bamboo under a sustained load; the results aim to provide a platform for future experimental work considering the creep of structural bamboo elements. By studying the phenomenon of creep on relatable materials, wood and composites, a fundamental understanding may be developed and hypotheses developed. The following sections develop these analogies to wood and composites.

1.3.1 Creep Behavior of Wood

The natural growth of bamboo results in material properties and behavior similar to those of wood. The strengths of wood and bamboo are affected by similar variables including: a) direction of loading in relation to the grain (fiber orientation); b) growth characteristics (i.e. knots, growth cycles, specific gravity, etc.); c) environmental conditions (i.e. moisture content, relative humidity, wet-dry cycles, temperature, etc.); and d) duration of load. Because of these similarities, creep tests performed on bamboo reflect the tendencies and performance of timber under sustained loads (Gaylord et al. 1997).

Creep is more susceptible in certain material than in others. For example, creep is considered common in wood, requiring a number of design factors and standards (Allen and Iono 2009). In design, the effect of sustained load is considered by expressing wood strength in terms of the wood's ten year strength. A permanent load, for example, may be designed for 90% of the ten year strength. Alternatively, the design for a rare impact load (by definition, not sustained) may consider 200% of the ten year strength. By plotting these two extreme conditions in collaboration with intermediate load cases, a more coherent visual representation of this concept becomes apparent (Fig. 1.2). In general, the usable strength of structural wood decreases as the duration of the load decreases.

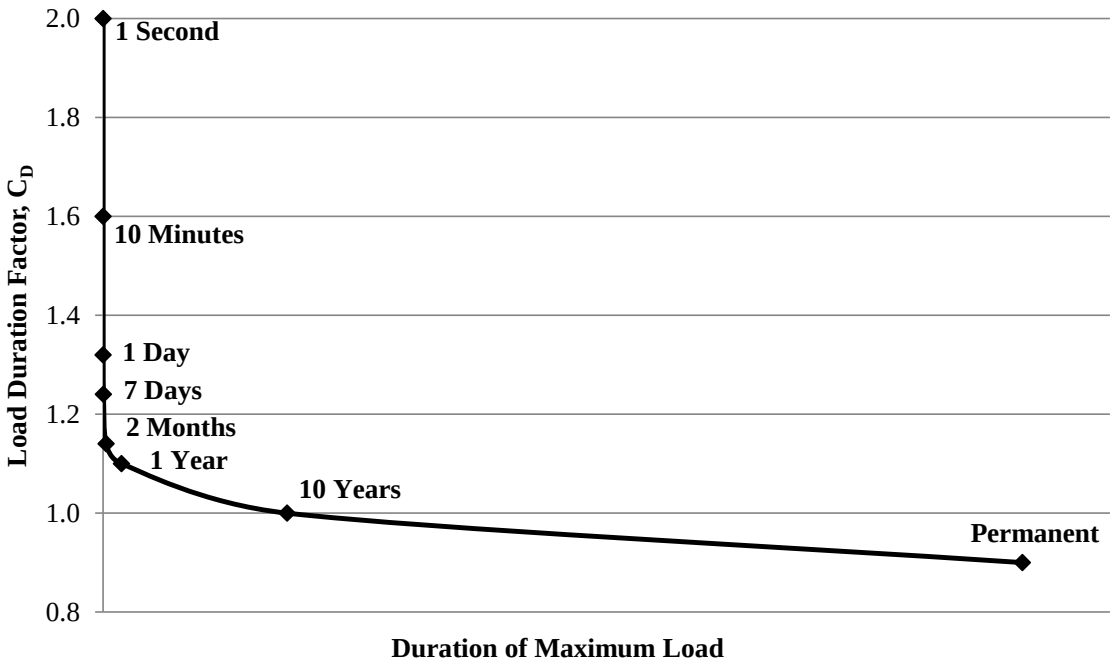

Figure 1. 2: Load duration factors for wood (adapted from ANSI, AF&PA NDS 2005).

1.3.2 Creep Behavior of Fiber Composite Materials

A composite, in its simplest form, may be defined as any material that is made up of more than one material. These materials are generally bonded, creating an interface. Composites may occur naturally, or they may be engineered (Hashin 1983). For this reason, bamboo may technically be categorized as a naturally-occurring fiber-reinforced composite consisting of the cellulosic fibers and lignin matrix. Additionally, based on the gradation of fiber in the culm wall, bamboo may be better described as a functionally-graded fiber-reinforced material. Therefore, understanding the effect of creep on unidirectional fiber composites becomes beneficial in the investigation of

bamboo under a sustained load. Study of creep effects in composites often focus on the difference in material properties of the fiber and the matrix. Similarly, creep effects consider the structure of the fibers within the matrix (Mileiko 1971). Both the emphasis on the relationship between the matrix and fibers and the fiber architecture translate well to the structure of bamboo.

Regardless of the specific materials that make up the matrix and reinforcement, concerns involving the effect of sustained loads remain unchanged. Creep of a composite material relies on the materials' individual properties as well as the properties of the composite as a whole. Each of the materials involved in the composite may creep individually, influencing the overall creep of the specimen. In most cases (at least those considering loads below the elastic limit of the material), it is assumed that the creep of the fiber is equal to the creep of the matrix. Therefore, the creep of each individual material equals the creep of the composite as a whole. This assumption is justifiable in composites that have continuous unidirectional fibers that run the entire length of the composite member. This simplifying assumption is adopted in the present work in which bamboo specimens are cut from an internode; these are expected to have continuous fibers through their length (this is not the case for a culm containing multiple nodes). In composites composed of short, rigid fibers, the structure must then be considered at both micro and macro scales. It must be recognized in the case of rigid fibers that the interaction of the separate materials impacts the susceptibility of the composite to creep. The interaction of the materials may have positive or negative effects on the creep strength in the scenario of rigid fibers (Lilholt 1985). The different bases for creep behavior based on the fiber architecture does raise the question: *will bamboo creep behavior differ when determined for small clear specimens than when determined for full-culm specimens?* The scope of the present work (presented in

Chapter 2), however, will only consider small clear[1] internode specimens subject to creep. The available research in this area is similarly limited.

Although the general reaction to sustained loads of engineered composites may be beneficial in predicting the behavior of bamboo, the natural growth and resulting structure of bamboo is more directly related to wood. So, while assumptions and predictions were based partially on the research performed within the field of composite structures, the testing standards developed for the experiment were adopted from wood design specifications.

1.3.3 Creep Behavior of Bamboo

The performance of bamboo as a structural material relies heavily on moisture content and creep. Although creep behavior of bamboo may be susceptible to loading parallel to the fibers, loads perpendicular to the fibers often govern general failure. Loads perpendicular to the fibers introduce a high risk of splitting. Splitting is commonly reported as the dominant mode of failure in bamboo members (Mitch 2010; Sharma 2010; Richard 2010).

In terms of the amount of lignin compared to the amount of cellulose, the composition of bamboo is similar to wood (Table 1.1). In Table 1.1, the crystallinity of a material refers to the weight fraction of crystalline cellulose, which affects the mechanical properties of cellulose fibers. More specifically, as crystallinity increases in bamboo or wood, the Young's modulus also increases (Andersson et al. 2003). Additionally, the creep of bamboo relies on its viscosity, which relies on the bamboo composition. Because of these relationships, the creep behavior of bamboo acts similarly to that of wood, and which is typically described by the Burgers-model

[1] Clear refers to a specimen free from gross strength affecting features such as knots, grain deviation, resin pockets and irregularities in the growth ring structure as defined for clear wood by Smith et al. (2003).

shown in Figure 1.3 (Janssen 1981). Janssen determined the permanent plastic deformation caused by creep in bamboo to be only 3-5% of the immediate deformation. Because of the insignificant effects of the sustained load, Janssen deemed creep in full-culm bamboo negligible. Although experimental evidence suggests that creep in bamboo is less than creep in wood, the variability of bamboo processing and storage may result in creep significantly different from the theoretical values obtained using a Burgers-model. In the present study, the drying process and initial storage conditions of the bamboo are unknown. Nonetheless, a Burgers model will be used to represent creep behavior. While absolute predictions may vary, it is believed that trends will be accurately represented.

Table 1. 1: Composition (percent) of bamboo and wood (adapted from Janssen 1981).

	Bamboo	**Deciduous Wood**	**Conifer Wood**
Cellulose	55	50	55
Other Polysacharides	20	25	15
Lignin	25	25	30
Mean Crystallinity	58	62	

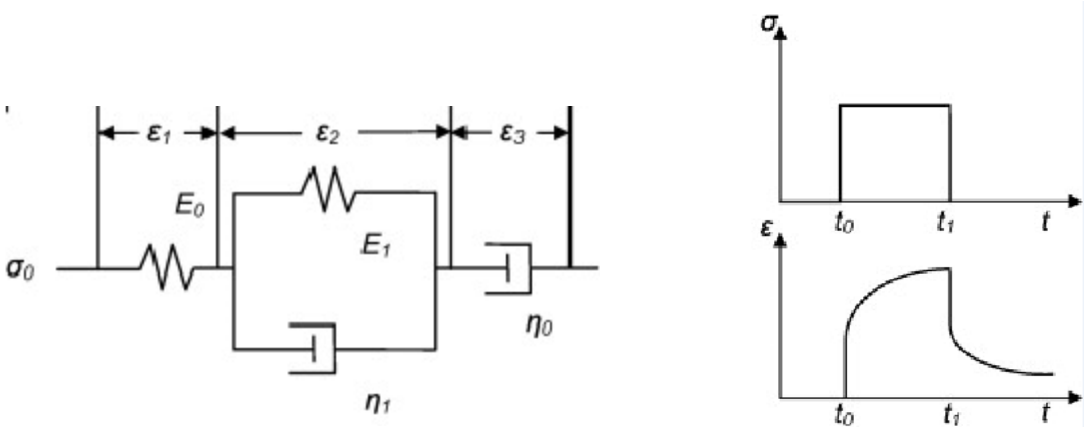

(a) Burgers-model (b) Creep and recovery curve

Figure 1.3: Burgers model (Liu et al. 2011).

Motivated by the necessity of trusses in practical construction, Janssen (1981) reports the large scale testing of bamboo trusses. “Truss 5” was 8 m long and had a 1:2 roof slope; it was tested under repeated loading to approximately 80% of its ultimate capacity (as determined from previous tests) to investigate creep and creep recovery. Midspan deflection (corresponding to the point of loading) was increased and released in five cycles over 380 days as shown in Figure 1.4. Janssen reports creep deformation as a result of compression, bending and shear and concluded that the deformation may be categorized into three ranges. The permanent deformation takes place in the viscous range and accounts for 49% of the total deformation. The immediate deformation occurs in the elastic range and accounts for 39% of the total deformation. Finally, creep takes place during the retarded elastic state and accounts for 12% of the total deformation. The creep recovery plot (Figure 1.4) for this experiment resembles a Burgers-model.

Figure 1. 4: Displacement time-history for Truss 5 showing creep and recovery (Janssen 1981).

On a smaller scale, creep deformation may be related to the structure of the bamboo. The creep behavior of the bamboo depends on the composition and fiber angle of the samples (Janssen 1981; Kanzawa et al. 2011). It has also been shown experimentally using clear flexural

specimens that the density of bamboo affects the initial deflection more than the long term creep of specimens (Kanzawa et al. 2011). Denser bamboo is stiffer, and therefore exhibits lower elastic deflection than less dense bamboo. Plastic deformation, on the other hand, was not apparently affected by fiber density. This hypothesis will be systematically tested in the present work by conducting flexural creep tests of specimens oriented such that either their denser, fiber-rich, outer culm wall or less dense inner culm wall are alternately placed in flexural tension.

In addition to the density, the shape of the vascular bundle has also been considered. The bundles at the outer radius of the bamboo tend to be more oval shaped, stretched in the radial direction (see Figure 1.1b). In contrast, the bundles located closer to the inside of the culm's cross section are more circular. The resulting fiber density and stiffness of the bundles due to the increased ratio of radial diameter to tangential diameter near the outer culm wall is found to have a less significant effect on creep deflection than on initial deflection (Kanzawa et al. 2011).

Kanzawa et al. (2011) showed experimentally, that initial deflection is more influenced by density than long term behavior. The small clear flexural specimens used for the experiment were cut from the full-culm in a tangential direction; the fiber gradation within each specimen is therefore not significant though the difference in density between specimens is significant. Initial deflection, shown in Figure 1.5, displays no difference between inner and outer portions of the culm wall. Compliance with respect to immediate behavior is a function of density only. On the other hand, long term creep strain (Fig. 1.5) affects less dense specimens (from the inner portion of the culm wall) differently than it affects denser specimens (from the outer portion of the culm wall). In all cases, creep tends to decrease as density increases. Because of this reoccurring trend, it is expected that the specimens with the fiber density in tension will perform better than the specimens with the fiber density in compression.

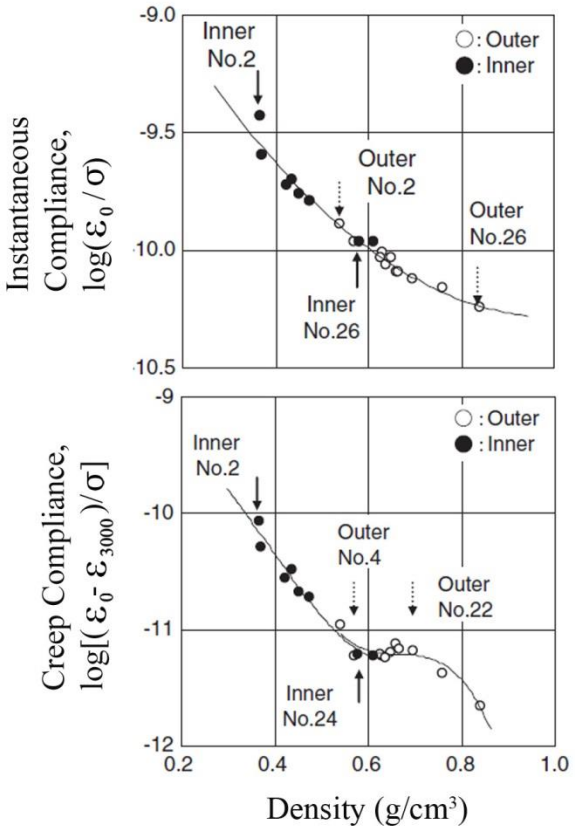

Figure 1. 5: Elastic and creep deflection versus density of Moso bamboo (adapted from Kanzawa et al. 2011).

Although the primary design of the current experiment (Chapter 2) will consider the relationship of creep and density proposed by Kanzawa et al. (2011), the results of the experiment performed by Obataya et al. (2007) are also taken into account since they are directly related in terms of specimen orientation. Obataya et al. suggested, based on four point bending tests of radial-cut specimens (similar to those used in the present study) that the best specimen orientation to increase flexural strength and deformability places the outer fibers in tension and inner fibers in compression. It is relatively well known that the specimen orientation will affect both the elastic and plastic behavior of bamboo under an initial load. However, the discovery of whether or not orientation affects the amount of creep experienced in bamboo specimens is of

interest in the present work. The results reported by Kanzawa et al. are somewhat contradictory on this issue. Although the specimen density is clearly shown to affect both initial deflection and creep deflection, the effect on the latter is significantly less. However, the specimen orientation clearly results in a discontinuity in the observed data.

The current study, presented in Chapter 2, intends to further the knowledge of the creep capacity of bamboo established by Kanzawa et al. while considering a specimen orientation similar to that used by Obataya et al. Half of the radially cut specimens subjected to a sustained load will be oriented so that the fiber density of the outer culm wall is in tension. The remaining specimens will be loaded so that the dense outer culm wall is in compression.

1.4 BAMBOO FLEXURAL TESTS

Four point bending tests of full-culm bamboo are one test standardized in the ISO bamboo materials test methods document (ISO 2004b). This standard test was based on the work and recommendations of Janssen (1981). In this test, failure is referred to as being flexural and the "modulus of rupture" or "flexural modulus" is calculated. In general, however, this is technically incorrect. Most full-culm bamboo, whether tested in flexure in the laboratory or performing *in situ* tends to exhibit a splitting mode of failure associated with longitudinal shear failure (Fig 1.6). This mode of failure has been the focus of much work conducted at the University of Pittsburgh (Mitch 2010; Sharma 2010; Richard 2013).

Longitudinal splitting occurs in bamboo for several reasons. The primary contributions to splitting include the weakness of the lignin matrix and inherent flaws (i.e. cracks from drying shrinkage, harvesting damage, etc.). Additionally, splitting is often initiated at connections, most

significantly at simple through-bolted connections (Fig. 1.6b) and at culm ends. It is believed that splitting or longitudinal shear failure is the most critical failure mode associated with many bamboo structural applications and methods of culm connection.

a) occurring in research b) occurring in practice (Sharma 2010)

Figure 1. 6: Longitudinal shear failure.

1.4.1 Previous Work

Richard (2013) initiated the investigation of longitudinal shear failure in bamboo culms under four point bending at the University of Pittsburgh. Among his conclusions were areas for potential future work including the need to consider short span culm bending tests and standard-span culm bending tests with longitudinal notches; both of which are addressed in this work in Chapter 3.

The ISO standard for full-culm flexure prescribes a specimen length at least thirty times the culm diameter based on the critical values for lateral strain. This length was determined theoretically by Vaessen and Janssen (1997) based on the specimen length resulting in simultaneous failure due to bending and shear stresses. In theory, at a shear span-to-depth ratio

of approximately 8.67, corresponding to a four point bending specimen length of 26D (where D is the culm diameter), failure due to maximum bending stress occurs in the compression zone while failure due to maximum shear stress occurs at the neutral axis. Thus to develop a flexural capacity, specimens having a span-to-depth ratio exceeding 10 (culm length of 30D) are recommended. This approach, however, neglects the apparently longitudinal shear-critical nature of full-culm bamboo in practice. Thus shorter shear spans may reveal more relevant material behaviors.

Two types of beam tests are conducted in the present work (Chapter 3) as a continued exploration of the longitudinal splitting behavior of bamboo beams; both short span specimens and specimens having longitudinal notch are considered. The procedure closely followed that developed by Richard, who tested standard 30D specimens with and without vertical notches, so that results may be directly compared. A brief summary of the results from Richard's work is presented below in order to familiarize readers with the background for the current experiments. Specific data from Richard's tests will be presented in Chapter 3 as required.

The initial set of tests conducted by Richard studied four scenarios: a) pure Mode I failure using the split pin tests developed by Mitch (2009); b) pure Mode II failure using the 'bowtie' test promulgated by ISO (2004a); c) full-culm mixed-mode failure investigated using modified four point flexure tests; and d) small scale clear specimen mixed-mode failure. These are described briefly in the following sections.

1.4.2 Mode I Failure

Mode I failure is the result of transverse opening tension (shown conceptually in Fig 1.7a). The transverse Mode I tension capacity of a bamboo culm may be determined using the split pin test developed by Mitch (2009). In general, the split pin test is repeatable (having a relatively low COV as reported by Mitch (2009) and Richard (2013)) and easy to conduct. The test, shown schematically in Figure 1.7c, involves the insertion of a split steel pin through a transverse hole with horizontal notches on either end. Richard conducted split pin tests on 4 inch diameter Moso and Tre Gai bamboo. A 25.4 millimeter (1 inch) diameter pin having additional 3 millimeter (0.12 inch) horizontal notches on both sides resulting in an overall flaw width 2a = 31.4 millimeters (1.24 inches) was used. The notches serve to initiate the failure in the horizontal (culm-longitudinal) plane. The steel pins are subjected to a tension load, pulling the pins away from each other until failure at the notch is initiated.

The resistance of bamboo to Mode I failure is based on its tensile strength perpendicular to the longitudinal fibers ($\sigma_{\perp}$); this often governs failure in practice. The Mode I tension capacity is calculated as:

$$\sigma_{\perp} = \frac{F}{2Lt - 4at} \tag{1-1}$$

Where F is the ultimate load measured at failure; L and t are the length and culm wall thickness of the specimen, respectively; and 2a is the total length of the initial notch. The recommended specimen length parallel to the fibers (L) is equal to the culm diameter (D) (Mitch 2009).

In addition to the perpendicular tension capacity, the split pin test provide values for the Mode I fracture toughness oriented in the culm-transverse direction, K_I, (Eqn. 1-2) and strain energy release rate, G, (Eqn. 1-3) of the bamboo.

$$K_I = \frac{F}{2Lt}\sqrt{\pi a}\left(\frac{L}{\pi a}\tan\left(\frac{\pi a}{L}\right)\right)^{1/2} \quad (1\text{-}2)$$

$$G_I = \frac{K_I^2}{E} \quad (1\text{-}3)$$

In which E is the elastic modulus in the transverse direction. Both values are measures of the toughness, or resistance to splitting, of the bamboo.

1.4.3 Mode II Failure

Mode II failure is the result of in-plane shear in the longitudinal direction of the culm (shown schematically in Fig 1.7b). For a bamboo culm, this capacity may be obtained using the 'bowtie' test developed by Janssen and promulgated by ISO (shown schematically in Fig 1.7d). The test involves the loading of a culm section in compression with bowtie plates. The plates are rotated with respect to each other so that the solid pieces of the top plate are opposite the solid pieces in the bottom plate. This results in the formation of four shear planes around the diameter of the culm. The resulting maximum shear stress (τ) based on the bowtie configuration is:

$$\tau = \frac{F}{\sum_{4Quadrants} Lt} \quad (1\text{-}4)$$

Where F is the ultimate load and L and t are the specimen height and wall thickness, respectively. The bowtie test is repeatable and simple to conduct. Although it is relatively practical in terms of performing the test itself, pure Mode II failure does not typically govern failure in bamboo. Because bamboo typically experiences a mixed-mode failure, the bowtie test

may better serve to provide values that will eventually be related to the mixed-mode capacity of a culm rather than simply the Mode II capacity.

1.4.4 Mixed-mode Failure

Potentially one of the largest issues in the study of longitudinal shear failure in bamboo is the relationship between the Mode I and Mode II failures. In a generic sense, failure under mixed-mode conditions may be expressed in the form:

$$\left(\frac{\sigma_{II}}{\sigma_{IICR}}\right)^{n}+\left(\frac{\sigma_{I}}{\sigma_{ICR}}\right)^{m}<1 \qquad (1\text{-}5)$$

Where σ_{II} and σ_{I} are the Mode II and I stresses and σ_{IICR} and σ_{ICR} are the critical Mode II and I stresses. The variables n and m are material-specific; both most simply taken as unity.

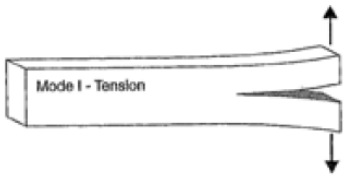

a) Mode I, opening tension (Smith et al. 2003)

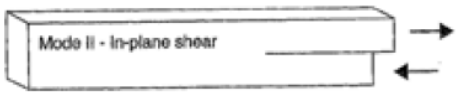

b) Mode II, in-plane shear (Smith et al. 2003)

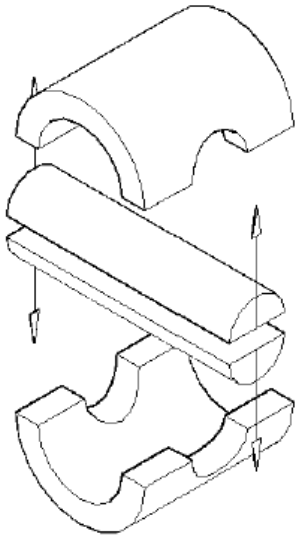

c) split pin test (Mitch 2009)

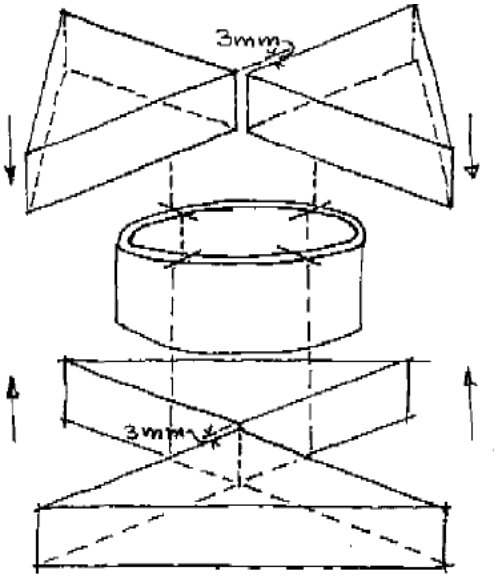

d) bow tie test (Janssen 1981)

Figure 1. 7: Fracture mode definitions and corresponding test methods.

In a flexural specimen subject to shear, there is a varying mode mixture along the shear span. As in most materials, the Mode II capacity is reduced in the presence of Mode I tension stresses. In longitudinally reinforced anisotropic materials, the Mode I strength and toughness may be orders of magnitude below the Mode II values. Therefore, as can be seen by applying Equation 1-5, the Mode II capacity may decrease rapidly in the presence of even a small amount of Mode I-oriented stress. It is of interest to develop a greater understanding of the individual and combined influences that each of the modes has on a flexure induced longitudinal shear failure. A summary of results reported by Richard (2013) is provided in Table 1.2. It is seen that the pure Mode II capacity is significantly greater than the pure Mode I capacity. The Mode II

capacities measured under conditions of mixed-mode loading seen in the bending specimens are apparently less than the pure Mode I capacity. This latter discrepancy of mixed-mode values may be due to the characteristics of the notch used in both the large and small scale bending tests. Because the transverse (vertical) notch extended from the tension face of each specimen to the neutral axis, the specimen capacities are significantly reduced. Indeed, it is felt that the notch geometry used does not permit a valid comparison of results. It is the contention of the present work that a longitudinal (horizontal) notch, serving only as a crack initiator, instead of a transverse notch is more appropriate for the study of mixed-mode splitting behavior. In addition, as is suggested at the conclusion of Richard's work, shorter span culms may be tested in order to witness and compare non-induced shear failure.

The present study, presented in Chapter 3, aims to continue the investigation of the relationship between Mode I tension and Mode II shear failures in a bamboo culm under four point bending. By performing modified variations of the previously conducted tests, a better understanding of the often-governing longitudinal shear capacity of bamboo is sought. The modifications will include a series of tests which decrease the shear spans of the culm uniformly in order to reduce the effect of flexural. The second modification is the placement of a horizontal (longitudinal) notch on the standard span culms. The notch will be located at midspan at the neutral axis.

Table 1. 2: Shear strength of Mode I, Mode II and mixed-mode failures (Richard 2013).

Species	Bowtie	Split Pin	Clear	Standard Span Tension Notch
	Mode II	Mode I	mixed-mode	mixed-mode
	τ, MPa (COV)	$\sigma_{\perp}$, MPa (COV)	τ, MPa (COV)	τ, MPa (COV)
Moso	14.20 (0.10)	2.40 (0.24)	1.82 (0.31)	1.82 (0.31)
Tre Gai	8.65 (0.075)	1.52 (0.16)	0.79 (0.26)	0.79 (0.26)
Normalized Values				
Moso	27.8	4.7	3.6	1.0
Tre Gai	26.2	4.6	2.4	1.0

1.5 SCOPE OF THESIS

This thesis addresses two separate issues relevant to the understanding of bamboo behavior and the eventual standardization of bamboo testing. Chapter 2 presents and a study of bamboo flexural creep behavior and the effects of sustained load on ultimate capacity. Small, clear specimens are used. These specimens are tested in flexure and alternately oriented such that the outer culm fibers are in tension or compression. Chapter 3 presents a continuation of the study initiated by Richard (2013) investigating the shear-flexure interaction and longitudinally splitting behavior of standard full-culm flexure tests. Each chapter will present the test programme, results and a discussion and conclusions for the individual test programmes. Chapter 4 will briefly summarize the conclusions and place the present study in the context of the larger goal of standardizing bamboo test methods.

2.0 CREEP TESTS

The experimental programme described in this chapter aimed to evaluate the creep behavior of *Bambusa Stenostachya* (Tre Gai) bamboo specimens under four-point bending. The experiment is motivated by the restriction of sustained load on various materials, particularly fiber reinforced materials, due to creep. Both wood and engineered composites are susceptible to damage caused by a sustained load. Long term strength of wood, for instance, is assumed to be about 55% of the short term strength (Janssen 1981). Long-term strength for glass fiber reinforced polymers (GFRP) may be as low as 20% (ACI 440.1 2006).

2.1 TEST PROGRAMME

Twenty five radially-cut small clear specimens were tested in this experimental programme (Table 2.1). All specimens were cut from the same culm of Tre Gai. Four specimens (N, S, E and W) were recovered from each of six adjacent internodes and numbered accordingly, as shown in Table 2.1 (additional specimens were cut from internode 1, as indicated in Table 2.1). Five specimens were initially tested to failure in order to determine an ultimate modulus of rupture. One unloaded control specimen was used to determine moisture content throughout the duration of the experiment. This specimen was stored with the creep specimens and included strain gages

in order to monitor any environmental effects; none were noted. Three additional specimens were stored, unloaded, in the test environment and tested in bending following the creep tests. The purpose of these three specimens was also to assess any effects of the storage environment over the duration of the creep tests (again, none) and to supplement the ultimate load values determined by the initial five control tests.

The sixteen remaining specimens were simultaneously subject to four point flexure (Figure 2.1) at various percentages of the ultimate load determined from the initially tested specimens and confirmed using beam theory. The nominal (target) specimen dimensions where width (*b*) of 12.7 mm (0.5 inches), height (*t*) of 12.7 mm (0.5 inches), and a clear span (*L*) of 213.4 mm (8.4 inches). The exact specimen dimensions depend on the nature of the culm and the specimen manufacturing process; the primary goal was consistency in dimension both within and between specimens. The greatest observed variation in dimension results from the change in wall thickness, or height of the beam (*t*), throughout the culm. Measured dimensions of all specimens are provided in Table 2.1.

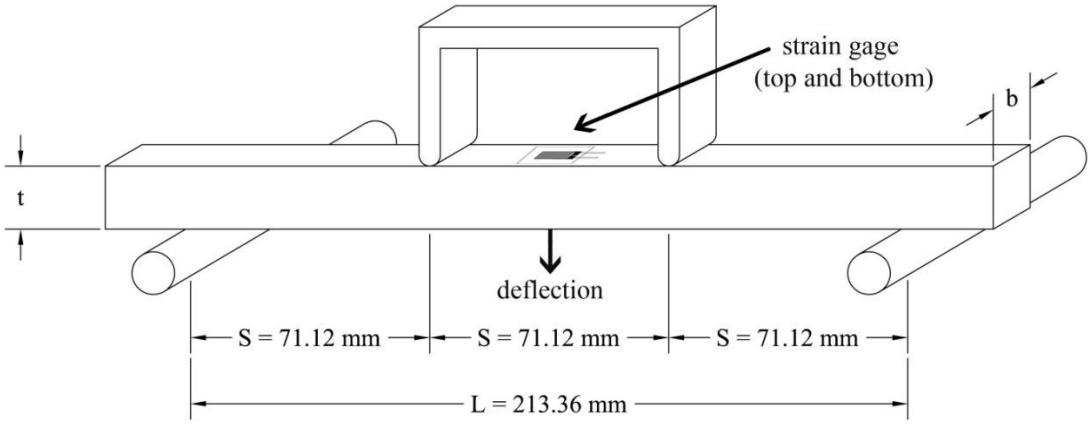

Figure 2. 1: Creep specimen dimensions.

The five control tests aided in the determination of an ultimate load capacity of the specimens, P_{ult} and provided a common value to be considered in each creep load determination. At the beginning of the creep test, specimens were loaded with target loads of $0.04P_{ult}$, $0.07P_{ult}$, $0.09P_{ult}$, $0.13P_{ult}$, $0.18P_{ult}$, $0.27P_{ult}$ and $0.40P_{ult}$ as indicated in Table 2.1. After 30 days of loading, four of the lightly loaded specimens (5S, 6N, 5E and 6W; see Table 2.1), initially having target loads of $0.04P_{ult}$, $0.07P_{ult}$, $0.09P_{ult}$, and $0.13P_{ult}$, were increased to values intended to represent $0.80P_{ult}$. These specimens were subsequently identified 5S*, 6N*, 5E* and 6W* (Table 2.1). The applied sustained creep loads and the actual proportion of P_{ult} for each specimen based on measured specimen dimensions are given in Table 2.1 and described in Section 2.1.2. For all subsequent calculations and discussion, the actual creep loads based on measured material properties are used.

It is ideal to machine the specimens from adjacent internodes within the same culm (Figure 2.2). The consistent origin of specimens allows for less variability in material properties. An additional effort to minimize variability requires each of the two specimens under a specific load to be oriented differently; one specimen should have its fiber-rich outer culm wall facing up (OC = outer fibers in compression), the other specimen should have its fiber-rich outer culm wall facing down (OT = outer fibers in tension). The difference in orientation of fiber density is shown in Figure 2.3. In this work, specimens with outer fibers in tension (OT) will be displayed in plots with solid lines, and specimens oriented with the outer fibers in compression (OC) are signified with dashed lines. Because of the interest in fiber density, it was important to maintain as much of the original culm wall thickness as possible despite the resulting inconsistency in specimen dimensions. In order to maintain accurate loading, the height dimension was minimally machined such that the opposing surfaces were parallel (Figure 2.2c) The variation in specimen

dimensions was normalized in the post-test analysis through the reporting of modulus of rupture (MOR), rather than specimen capacity. Because of the consistency provided by the machining of the specimens, the clear span of each bamboo specimen did not vary. Similarly, the machined width of the creep beams is relatively constant at b = 12.37 mm with a coefficient of variation (COV) of 0.036. The naturally occurring wall thickness (depth of the beam) varied more significantly with t = 14.34 mm (COV = 0.12). In addition to dimensions, alignment of the specimen was made consistent with that specified by ASTM E2714 *Standard Test Method for Creep-Fatigue Testing*.

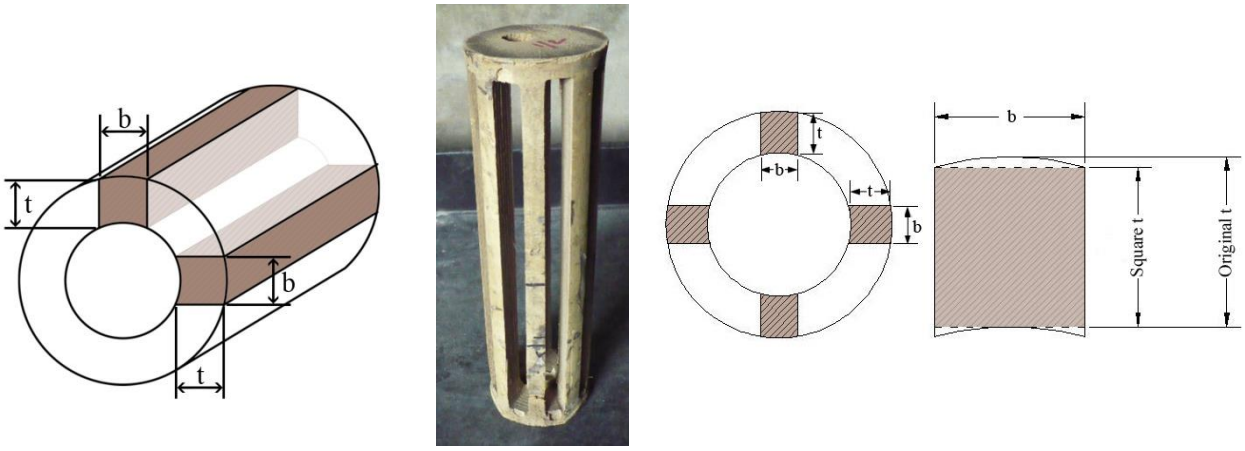

a) specimens cut radially from internode

b) internode 1 following specimen machining

c) machined dimension of specimen

Figure 2. 2: Test specimen machining.

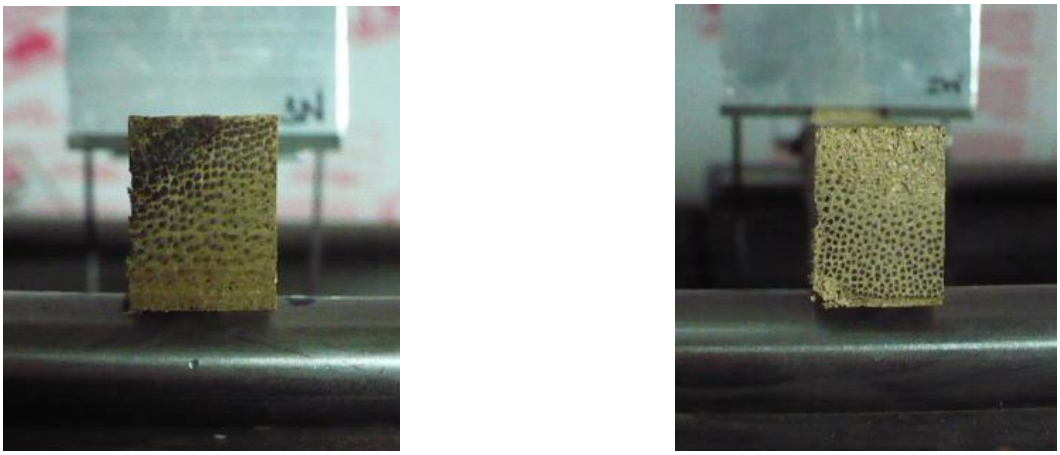

a) outer fiber density in compression (OC) b) outer fiber density in tension (OT)

Figure 2. 3: Test specimen orientation.

2.1.1 Creep Load Assembly and Test Protocol

The creep loading assembly is shown in Figure 2.4. Free weights were used to apply the sustained load. The free weights were placed on an eye hook which then transferred the weight to a C-channel through a wire. Although the weights hung at different heights in order to accommodate spacing restrictions, each wire was cut to the same length and thus the assembly weight in each case was constant (5.0 N). The loading and support locations must be undamaging to the bamboo. The assembly includes two sets of continuous roller supports, each supporting eight specimens (Fig 2.4d). The 12.7 mm (0.5 inch) diameter rollers, set at a clear span of 213 millimeters (8.4 inches), are supported on a steel grate allowing the wire transferring the load to easily attach to the channel acting directly on the bamboo. The channel allowed the load to be distributed in four point bending having a fixed constant moment region of 71 millimeters (2.8 inches) as shown in Figure 2.1. The edges of the channels were rounded to a 2.5

mm (0.10 in.) radius. In order to minimize impact during application of the free weights, a small scissor jack was used to lift the weights onto the eyehooks.

Based on the protocol reported in ASTM D6815 *Standard Specification for Evaluation of Duration of Load and Creep Effects of Wood and Wood-Based Products*, the sustained load was applied for 90 days or until failure. The vertical deflection at midspan (Fig 2.1) was measured using a digital depth gauge (Fig 2.4f) using the bottom of the fixed grate as a reference. Strain gauges applied to the top and bottom surfaces of the specimens in the constant moment region (Fig 2.1) captured extreme fiber compression and tension strain, respectively, and were used to calculate curvature and the location of the neutral axis. All data was collected a) immediately prior to loading; b) immediately following loading (elastic displacement and strain); c) every 15 minutes for the first hour; d) every 30 minutes for the next eleven hours; e) twice a day for the subsequent six days; and f) daily after that. Load was removed at 90 days at which point additional readings were taken. Specimens were permitted to 'relax' for ten days prior to final testing to failure. During this relaxation time, data was recorded a) immediately after the load was removed; b) every 15 minutes for the first hour of recovery; c) every hour for the following 6 hours and d) daily thereafter.

As noted previously, following 30 days of loading (and relatively little creep), four lightly loaded specimens (5S, 6N, 5E and 6W) had additional free weights applied to increase their creep loads. The protocol was restarted at this time for these specimens. Thus these four specimens were under relatively small loads for 30 days (5S, 6N, 5E and 6W) followed by higher loads for an additional 90 days (5S*, 6N*, 5E* and 6W*). The dramatic change in load at 30 days is clearly evident in all data for these specimens.

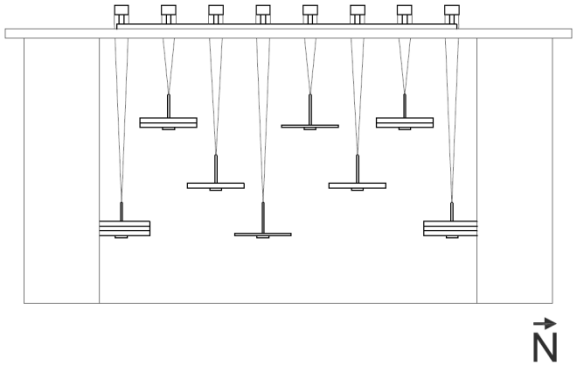

a) section view of test configuration

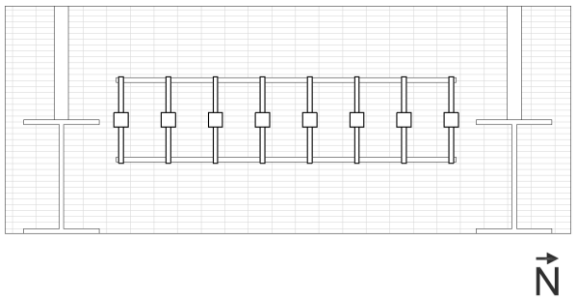

b) plan view of test configuration

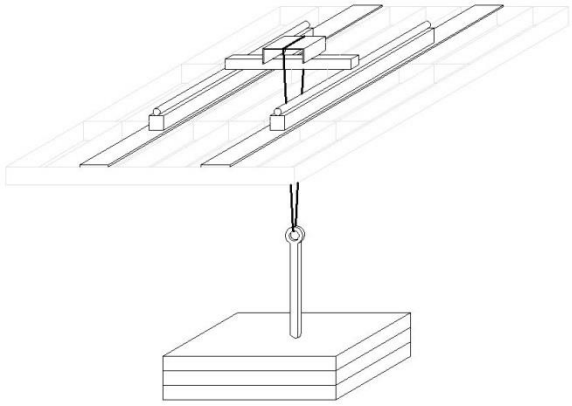

c) axonometric detail of test configuration

d) continuous supports

e) complete test set-up

depth gauge

f) caliper

Figure 2. 4: Test configuration.

Table 2. 1: Test specimen matrix.

Specimen Identification and Parameters							Creep Test Results										Residual Strength Following Creep Testing				
Specimen		Fiber Density	Width	Height	Neutral Axis	Target Creep P_{ult} ratio	Applied Creep Load	Actual Creep P_{ult} ratio	Applied Average MOR (Eq. 2-1)	Initial Defl.	Normalized Deflection			Relative Creep			Creep Recovery	Ult. Load	Top of Beam MOR (Eq. 2-2)	Bottom of Beam MOR (Eq. 2-3)	Max Defl.
			b	T	α		P		f_r	D_1	D_{30}	D_{60}	D_{90}	RC_{30}	RC_{60}	RC_{90}		P_{ult}	f_t	f_b	D_{max}
			mm	Mm			N		MPa	mm	720 hours	1440 hours	2160 hours	720 hours	1440 hours	2160 hours		N	MPa	MPa	mm
Creep Specimens	2N	OC	12.90	16.89	0.63	0.40	267	0.39	15.47	3.21	1.02	1.06	1.06	0.10	0.11	0.13	0.97	1468	62.72	107.44	8.96
	2S	OC	12.83	12.47	0.58	0.40	267	0.79	28.57	5.11	1.26	1.30	1.32	0.39	0.43	0.46	0.75	667	61.09	81.77	9.09
	3N	OC	12.45	16.71	0.64	0.27	178	0.30	10.92	2.93	1.09	1.14	1.15	0.19	0.22	0.25	0.95	1157	54.14	87.85	6.55
	4N	OC	12.98	12.26	0.62	0.27	178	0.56	11.92	2.58	1.16	1.15	1.19	0.20	0.26	0.29	0.94	1379	72.99	111.81	11.23
	5N	OC	12.19	12.26	0.59	0.13	89	0.29	10.37	3.18	1.02	1.09	1.12	0.14	0.17	0.20	0.97	667	66.65	88.83	11.88
	5S	OC	12.19	13.26	0.65	0.13	89	0.24	8.87	2.28	2.19	2.22	2.27	0.12	--	--	--	--	--	--	--
	5S*	OC	12.19	13.26	0.63	1.00	356	0.98	35.46	4.37	1.16	2.19	2.22	3.59	3.69	3.90	0.89	1157	144.68	85.82	11.20
	6N	OC	12.12	14.62	0.67	0.07	44	0.10	3.67	1.33	3.21	3.22	3.19	0.20	--	--	--	--	--	--	--
	6N*	OC	12.12	14.62	0.63	1.00	356	0.81	29.33	3.56	1.42	3.21	3.22	6.91	7.11	7.19	0.85	1290	84.59	128.04	10.09
	6S	OC	11.86	14.22	0.59	0.07	44	0.11	3.96	2.21	0.98	1.01	0.97	0.09	0.16	0.23	0.86	890	62.51	95.76	10.14
	2E	OT	13.28	14.00	0.22	0.27	267	0.41	21.91	3.07	1.13	1.19	1.21	0.28	0.32	0.33	0.83	1272	121.69	82.76	18.91
	2W	OT	12.73	17.81	0.39	0.27	267	0.28	14.12	2.52	1.00	1.08	1.08	0.13	0.18	0.18	0.93	1779	106.35	63.08	23.13
	3E	OT	12.04	14.59	0.40	0.18	178	0.30	14.81	2.16	1.28	1.41	1.44	0.32	0.38	0.41	0.83	1112	115.36	69.74	20.74
	4E	OT	12.12	14.44	0.16	0.18	178	0.22	15.04	2.48	1.40	1.45	1.46	0.63	0.72	0.76	0.68	1068	114.50	65.92	22.24
	5E	OT	12.34	12.42	0.44	0.09	89	0.80	9.98	1.83	5.04	5.24	5.49	0.34	--	--	--	--	--	--	--
	5E*	OT	12.34	12.42	0.40	0.80	356	0.80	39.91	5.94	1.33	5.04	5.24	3.80	4.46	5.06	0.67	876	99.84	96.72	15.88
	5W	OT	12.07	14.99	0.48	0.09	89	0.14	7.01	1.58	1.42	1.49	1.52	0.09	0.09	0.07	0.80	1112	108.81	66.41	15.81
	6E	OT	11.91	13.18	0.40	0.04	44	0.09	4.59	1.49	1.43	1.65	1.64	0.10	0.10	0.11	0.92	934	123.73	69.11	18.27
	6W	OT	11.86	15.30	0.43	0.04	44	0.07	3.42	1.47	2.94	2.97	3.14	-0.17	--	--	--	--	--	--	--
	6W*	OT	11.86	15.30	0.40	0.80	356	0.55	27.36	3.71	1.45	2.94	2.97	7.61	7.92	8.81	0.85	1739	135.71	76.33	19.91
Control Specimens	1N	OC	6.48	17.27	0.65													792	51.64	94.57	4.03
	1S	OC	6.07	15.47	0.61													610	58.41	91.24	3.98
	3S	OC	12.45	12.22	0.58													721	68.77	96.68	10.31
	4S	OC	13.28	15.52	0.62													807	40.97	66.93	8.83
	1NE	OT	6.43	16.36	0.39													1039	131.75	83.48	9.53
	1SE	OT	6.86	13.16	0.36													822	158.52	87.70	11.98
	1SW	OT	6.78	16.94	0.30													1157	148.01	63.66	11.70
	4W	OT	12.24	16.59	0.40													1072	81.01	54.81	27.74

2.1.2 Control Tests and Results

An aim of this experimental programme is to consider the orientation of the fiber density. At each creep load value, two samples are oriented so that their outer culm-wall fibers are in compression (OC) and two are oriented so that their outer culm-wall fibers are in tension (OT).

The control bending tests (see bottom of Table 2.1), conducted prior to the initiation of the creep tests, allowed for proper sizing and loading of the specimens. Five radially-cut specimens were tested (Figure 2.2); three in the OT orientation and two in the OC orientation. The specimen dimensions varied somewhat from the uniform creep specimens (Table 2.1) however capacities were normalized by the dimensions by considering and comparing the modulus of rupture (MOR), rather than specimen load carrying capacity.

Following the creep tests, an additional three specimens (3S, 4S and 4W in Table 2.1) were tested verifying the results from the initial five tests. The cross sections of the three specimens in the second set of control tests were closer to those of the creep test specimens and larger than the cross section of the original five tests.

All control tests were tested monotonically to failure in a test arrangement identical to that used for the creep conditioning (Figure 2.1). Instrumentation was also the same in all cases. Testing was conducted in displacement control and data taken at increments of approximately 44 N applied load.

In general, specimens that were loaded with the outer culm-wall fibers in tension (OT) carried more load and exhibited greater midspan deflection than the specimens that were loaded with the outer fibers in compression (OC). This is shown in Figure 2.5, in which solid lines represent the OT specimens and dashed lines represent the OC specimens (this notation is

consistent for all reported results). The midspan deflection for all specimens tested monotonically to failure is the displacement experienced by the crosshead of the machine. Based on the strain readings taken from the compression and tension faces throughout the test, shown in Figure 2.6, the location of the neutral axis of the specimens may be calculated. The OC specimens exhibited an upward shift of the neutral axis (relative to the specimen centroid at t/2) toward the compressive face of the specimen (Fig. 2.7a) while the OT specimens exhibited the opposite shift: downward, toward the tension face (Fig 2.7b). In both cases, the shift from the centroid was about 10 to 15% of the specimen height. The location of the neutral axis given in terms of a proportion of the specimen height measured from the bottom (tension) face, αt is given in Table 2.1. The evaluation of neutral axis location, discussed more thoroughly in section 2.3.2, is considered when calculating the separate modulus of rupture (MOR) values for the top and bottom of the each beam.

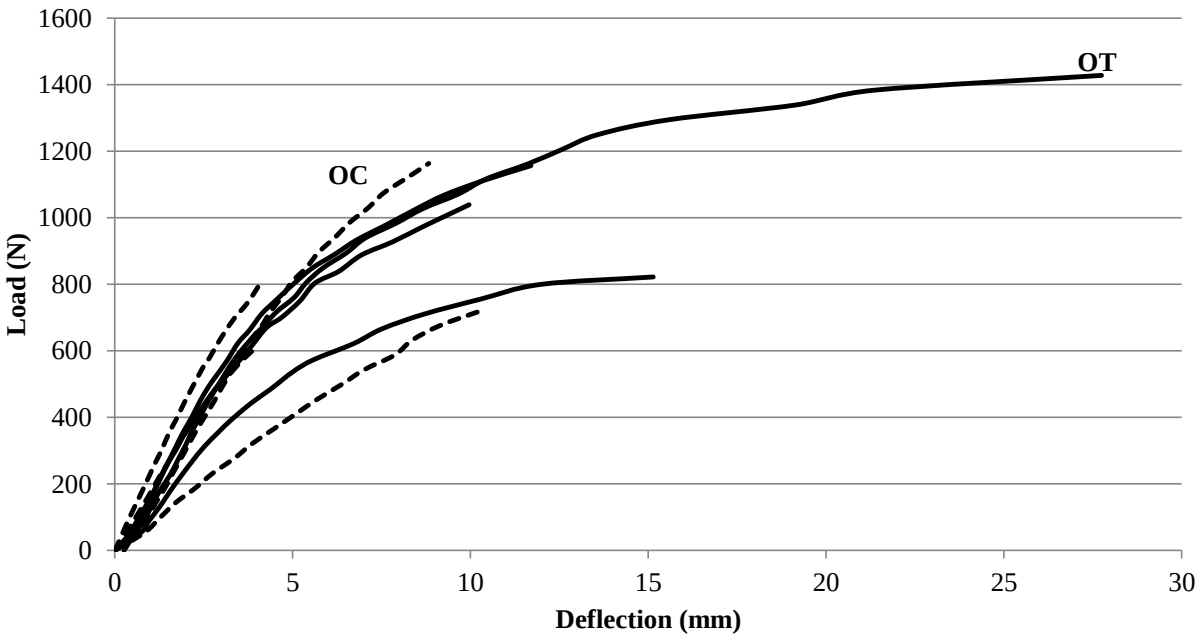

Figure 2. 5: Load versus displacement.

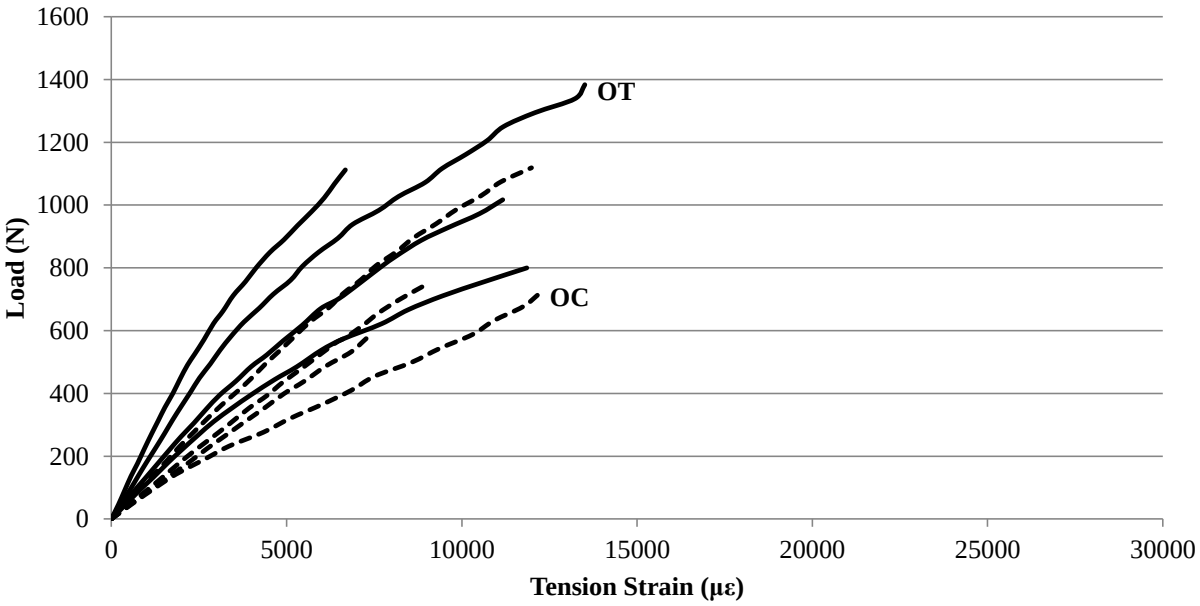

(a) tension strain

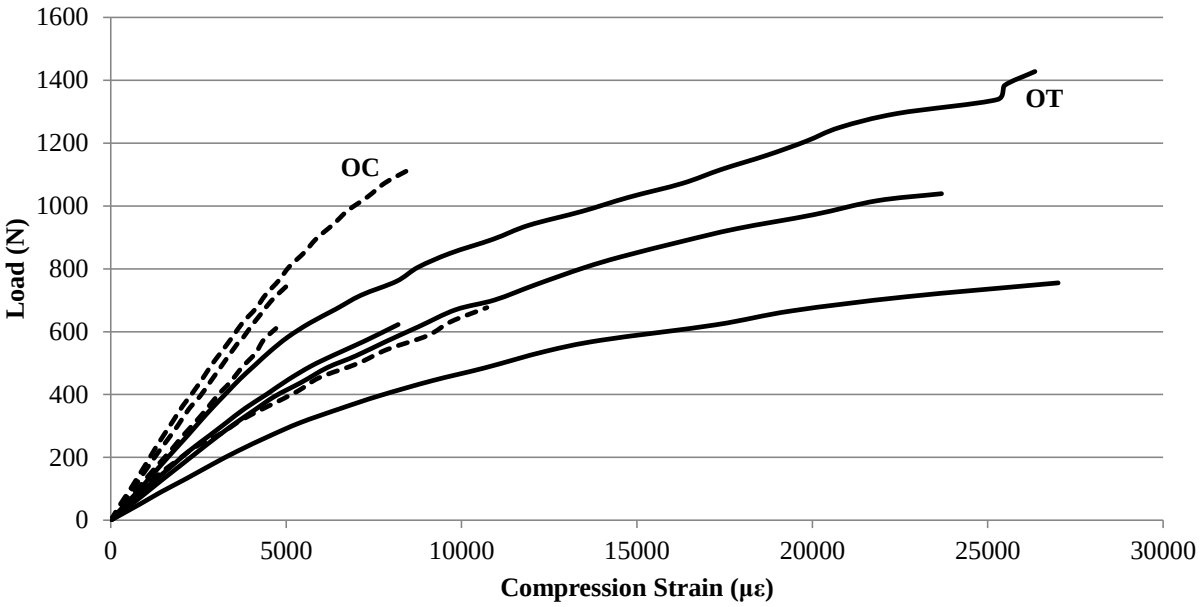

(b) compression strain

Figure 2. 6: Load versus strain.

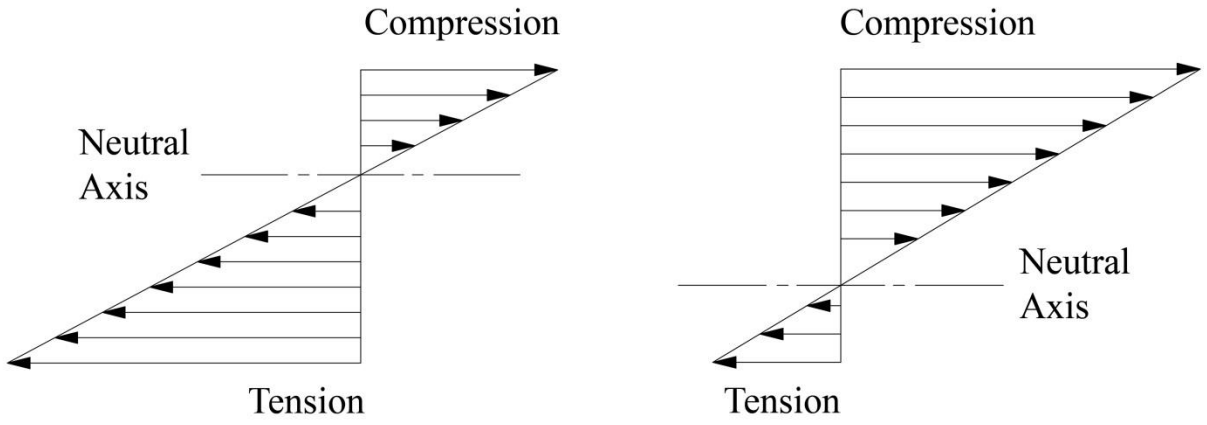

(a) OC specimens **(b)** OT specimens

Figure 2. 7: Location of neutral axis.

It can be seen in Figure 2.6 that the OT specimens experienced higher compression and tension strains (resulting from larger capacities and deflections as shown in Figure 2.5), although specimen orientation had a greater impact on the compression strain data.

Failure modes were affected by specimen orientation. OC specimens failed primarily perpendicular to the fibers at the tension face (Fig 2.8a). The low fiber density at the tension face permitted tension failure to develop in the lignin matrix. The OT specimens exhibited a 'brooming' failure typical of fiber reinforced materials having a large fiber volume (Fig 2.8b). In this case, individual fibers initiate the rupture sequence. The fracture zone of individual fibers is spread over the constant moment region and no clear 'crack' or failure plane is evident. Due to the low transverse strength properties, as the fracture zone moved up, away from the tension face, the specimens began splitting in longitudinal shear. The residual capacity of the specimens is considerably more flexible and the specimens continue to resist load. Final failure was defined when either the load dropped below 50% of the ultimate capacity or the specimen 'bottomed out' in the test apparatus (also seen in Fig 2.8).

(a) OC specimen **(b)** OT specimen

Figure 2. 8: Typical flexural failures.

The modulus of rupture (MOR), f_r, is calculated based on the ultimate capacity for each specimen as follows:

$$f_r = \frac{My}{I} = \left(\frac{Pa}{2}\right)\left(\frac{t}{2}\right)\left(\frac{12}{bt^3}\right) \tag{2-1}$$

Where $M = Pa/2$ is the applied moment in which P is the ultimate applied load (Fig. 2.5) and a is the shear span, equal to 71 mm in all cases (Fig. 2.1).

$y = \frac{t}{2}$ is the location of the specimen centroidal axis.

$I = \frac{bt^3}{12}$ is the moment of inertia of the specimen section

The calculation given by Equation 2-1 is commonly reported in the literature and represents an apparent average value of MOR. However, to understand the effects of specimen orientation, it is necessary to consider the MOR calculated for both the top and bottom extreme fibers. This is done by recognizing the shift from the centroid of the neutral axis (Fig. 2.7) and replacing $y = t/2$ in Eq. 2-1 with $y_t = (1-\alpha)t$ and $y_b = \alpha t$, thus:

$$f_t = \frac{My_t}{I} = \left(\frac{Pa}{2}\right)\left((1-\alpha)t\right)\left(\frac{12}{bt^3}\right) \tag{2-2}$$

$$f_b = \frac{My_b}{I} = \left(\frac{Pa}{2}\right)\left(\alpha t\right)\left(\frac{12}{bt^3}\right) \tag{2-3}$$

Where the location of the neutral axis given in terms of a proportion of the specimen height measured from the bottom (tension) face, αt is given in Table 2.1. Using the MOR allows normalization for variation in specimen geometry.

Table 2.2 summarizes the MOR calculations for the five control specimens tested prior to creep testing and the three tested following creep testing. The initial five tests had nominal dimensions of approximately t = 16 mm and b = 6.5 mm. These were used to select specimen

dimensions for the creep tests that would correspond approximately to the desired target load levels considering that only discrete 4.54 and 9.09 kg free weights were available. With the culm wall thickness, *t*, established, a nominal specimen width *b* = 12.5 mm was selected for creep testing. The three subsequently tested control specimens (Table 2.2) had the same nominal dimensions as the creep tests. The target creep load levels and those actually tested, along with measured specimen dimensions are provided in Table 2.1.

Table 2. 2: Average modulus of rupture values.

Orientation	Pre-Creep Control Tests			Post-Creep Control Tests		
	f_r	f_t	f_b	f_r	f_t	f_b
	(MPa)	(MPa)	(MPa)	(MPa)	(MPa)	(MPa)
OC	74.0	55.0	92.9	68.3	54.9	81.8
OT	112.2	146.1	78.3	67.9	81.0	54.8
all	96.9	109.7	84.1	68.2	63.6	72.8
Standard Deviation (COV)						
OC	1.2 (0.016)	4.8 (0.087)	2.4 (0.025)	20.3 (0.298)	19.7 (0.358)	21.0 (0.257)
OT	9.5 (0.085)	13.5 (0.092)	12.8 (0.164)	-	-	-
all	22.0 (0.227)	50.8 (0.464)	12.2 (0.145)	14.4 (0.211)	20.5 (0.323)	21.5 (0.296)

2.1.3 Creep Test Environment

The location where the creep tests were conducted was required to have consistent humidity throughout the entire testing period. Based on ASTM D6815-09, the environment should be considered ‘dry service conditions’; for timber creep tests the moisture content of the wood should not exceed 19%. The average moisture content of the bamboo (measured using an Extech Instrument MO220 moisture meter) throughout the experiment was 12%.

The ambient environmental conditions were measured each day a reading was taken as reported in Figure 2.9. Additionally, an unloaded ‘traveler’ specimen was instrumented with

strain gages in order to monitor the strain generated from changes in environment. The ambient temperature remained very constant at 20.8^{o}C. The relative humidity varied between 40 and 60% having an average of 53%. Finally, no significant strain variation was seen in the instrumented 'traveler' specimen. The recorded ambient environmental conditions were both constant and typical of 'dry service conditions' and are therefore not expected to have affected the creep behavior in any way.

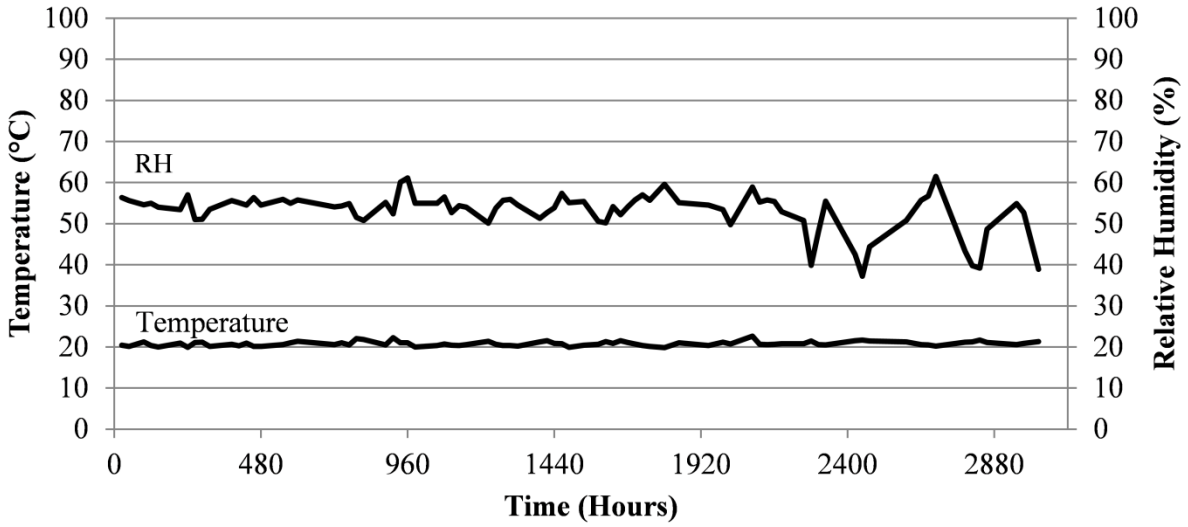

Figure 2. 9: Variation in environmental factors.

2.2 CREEP TEST RESULTS AND DISCUSSION

A summary of key creep test results is provided in Table 2.1. In general, the difference in orientation and load yielded expected results. The amount of deflection and the location of the neutral axis followed the trends established in the control tests. The three additional specimens tested in bending also confirmed previous conclusions. No specimens exhibited creep rupture over the 90-day monitoring period. Following 30 days, the load applied to four lightly loaded

specimens (5E, 5S, 6W, 6N) was increased in an attempt to drive a creep failure due to the sustained load. These specimens were designated 5E*, 5S*, 6W*, 6N* and were subjected to the increased loads for 90 days, resulting in their being under load for a total of 120 days. Still, no creep rupture failures resulted, although the data captured a wider range of response. The increase in applied load is very clear on all plots at an elapsed time of 30 days (720 hours) and should be considered when viewing the results.

2.2.1 Deflection and Strain

Creep deflection versus time under load is shown in Figure 2.10. In Figure 2.11 and in Table 2.1, creep deflections are normalized by the initial deflection measured upon application of the load. Some caution must be taken in interpreting the *unnormalized* results shown in Table 2.1. While the absolute initial deflection values for the OC specimens (average = 3.1 mm) exceeds that of OT specimens (2.6 mm), this must be viewed in light of the fact that due to the differences in capacity based on orientation, the applied creep load ratios are also considerably higher for the OC specimens (average = $0.46P_{ult}$) than for the OT specimens ($0.37P_{ult}$). Indeed, consistent with the control tests, the apparent initial stiffness of both orientations is similar.

Based on the normalized deflections (Fig. 2.11), creep deflection can be seen to be clearly affected by specimen orientation. In general OT specimens exhibit greater normalized creep than OC specimens. Values of normalized deflection at 30, 60 and 90 days are given in Table 2.1. This trend may be due to the flexibility of the specimens based on their orientation. Section 2.2.2 discusses the difference in apparent modulus of elasticity of OT and OC

specimens. Generally OC specimens have a higher modulus perhaps resulting in less plastic creep deformation.

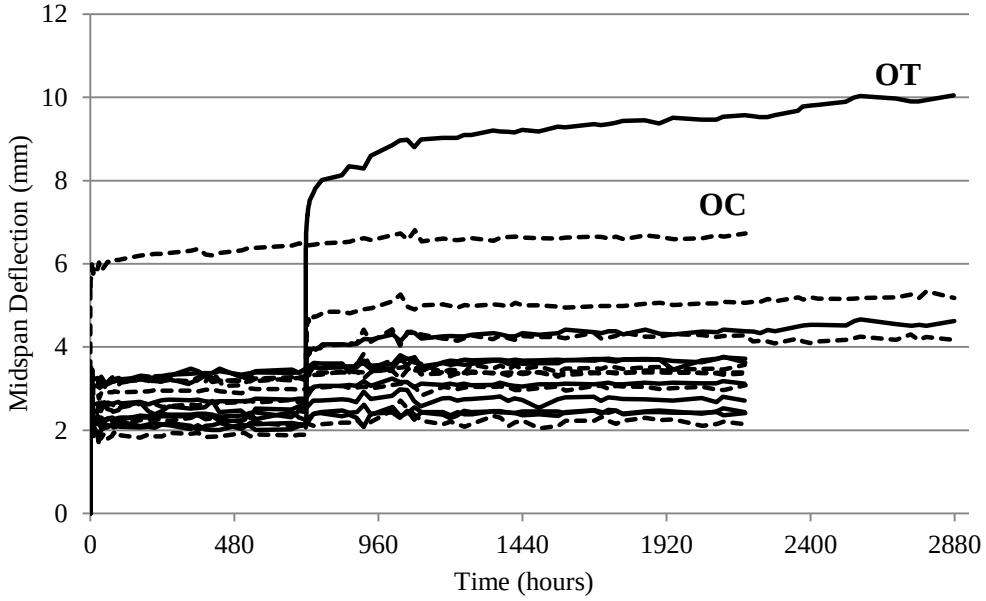

Figure 2. 10: Creep deflections.

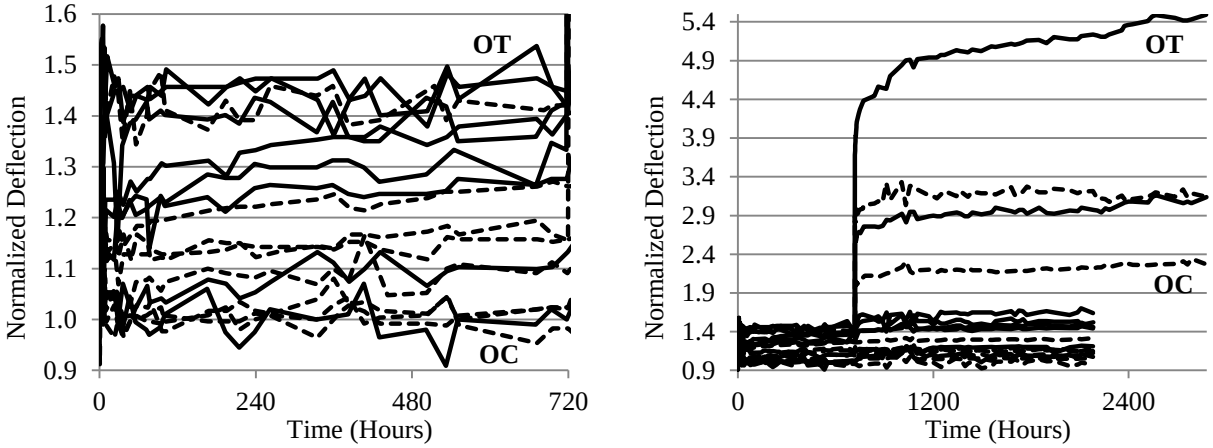

a) first 30 days b) entire 120-day creep programme

Figure 2. 11: Normalized creep deflections.

2.2.2 Apparent Young's Modulus

The apparent modulus of elasticity, $E_{apparent}$, or Young's Modulus, for the bamboo specimens may be obtained as:

$$E_{apparent} = \frac{PL}{144I\Delta}\left[3L^3 - \left(\frac{4L}{3}\right)^2\right] \quad (2\text{-}4)$$

Where P is the applied load; L is the clear span; I is the moment of inertia of the specimen; and Δ is the initial elastic deflection at midspan corresponding to the application of P. Similar to wood, the key material properties of bamboo are strictly apparent values due to the inherent material variation and the presence of flaws. Although the apparent modulus may vary by sample, the values are determined from a wide range of specimens, creating a more empirical value based on dimension and orientation.

The overall apparent modulus of elasticity based on the data recorded at the initial application of the creep loads was 31527 MPa (4573 ksi; COV = 0.268). When considered with respect to specimen orientation, the modulus of elasticity calculated for OC specimens was 36236 MPa (5256 ksi; COV = 0.210) while an average value of 26818 MPa (3890 ksi; COV = 0.255) was determined for OT specimens. These values were obtained using the data collected from only the 12 specimens subjected to a target creep ratio greater than $0.07P_{ult}$. The four specimens subject to the smallest loads (with target ratios of $0.04P_{ult}$ and $0.07P_{ult}$) exhibited very little deflection affecting the precision of the calculation. Based on the data, the orientation of the clear specimen does appear to affect its stiffness, contrary to the conclusions of Obataya et al. (2007) reported in section 1.2. Although the discussion presented by Obataya et al. does not consider the difference in stiffness among orientations significant, it is shown in their data that

OC specimens have an apparent modulus of elasticity approximately 6% higher than the modulus of OT specimens. The larger modulus seen in OC specimens is consistent with the current test results. Therefore, it is that orientation of clear specimens affects both stiffness and flexural deformability.

2.2.3 Creep Strain and Relative Creep

Strains measured on the top (compressive) and bottom (tension) faces of each specimen are shown in Figure 2.12. These illustrate similar trends as the creep deflections described previously. Figures 2.12a and c indicate that OT specimens typically exhibit a significantly higher compressive strain than OC specimens. Although the difference is less significant with respect to tension strains, Figures 2.12b and d show that OC specimens generally exhibit higher tension strains than OT specimens. These results were expected and directly correlate to the strength of the fibers, especially when the fibers are carrying primarily tension loads.

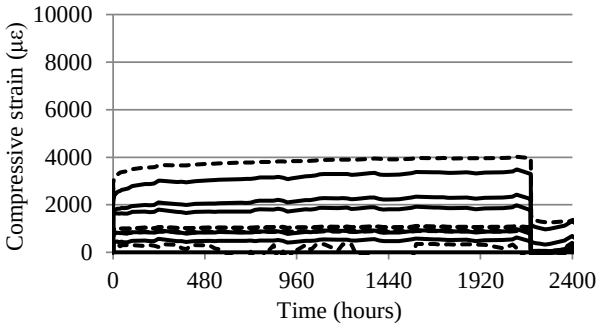

a) compressive creep strains (shown as positive) for specimens having no load increase

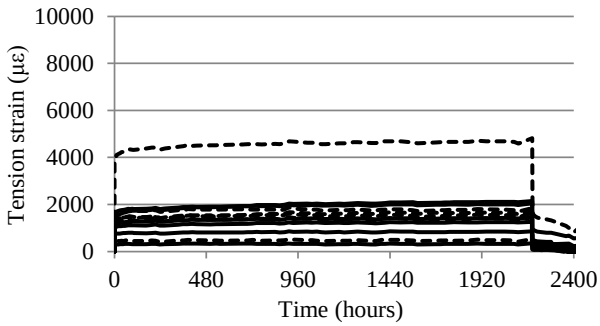

b) tensile creep strains for specimens having no load increase

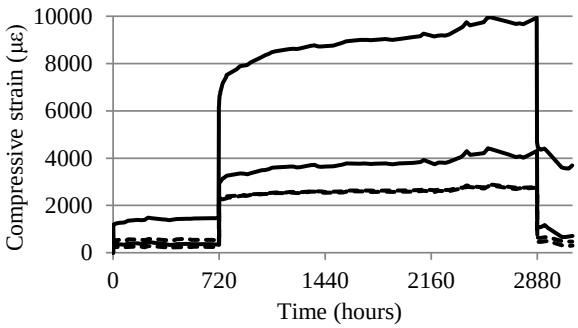

c) compressive creep strains (shown as positive) for Specimens 5S, 6N, 5E and 6W

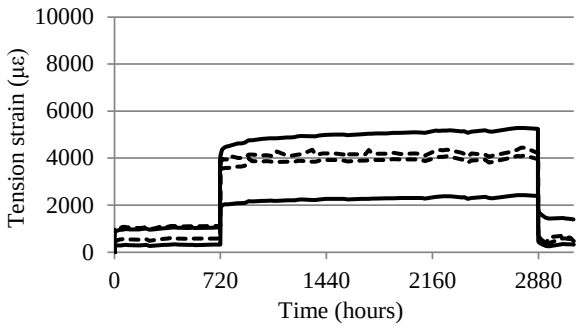

d) tensile creep strains for Specimens 5S, 6N, 5E and 6W

Figure 2. 12: Creep strains.

A method of normalizing measured creep strains is to consider the relative creep (RC), determined as:

$$RC = \frac{\left(\varepsilon(t) - \varepsilon_0\right)}{\varepsilon_0} \tag{2-5}$$

Where $\varepsilon(t)$ is the strain at time t and ε_0 is the initial strain. Table 2.1 provides values of relative creep at 30, 60 and 90 days calculated using the average absolute values of the tension and compression strains. This data clearly reveals a decreasing creep rate with time under load.

Smith et al. (2003) describes the three stages of creep behavior: primary, secondary and tertiary as shown in Figure 2.13. Primary creep takes place over a relatively short period of time and is associated with redistribution of elastic load. Thus, the primary creep stage is expected to be more pronounced for larger sustained loads. For small sustained loads, the primary creep stage may be virtually nonexistent. The tertiary creep stage represents imminent failure of the member (specimen) and usually indicates progressive failure of the material. The secondary stage is less determined and its duration is a function of material properties, geometry and the level of sustained load.

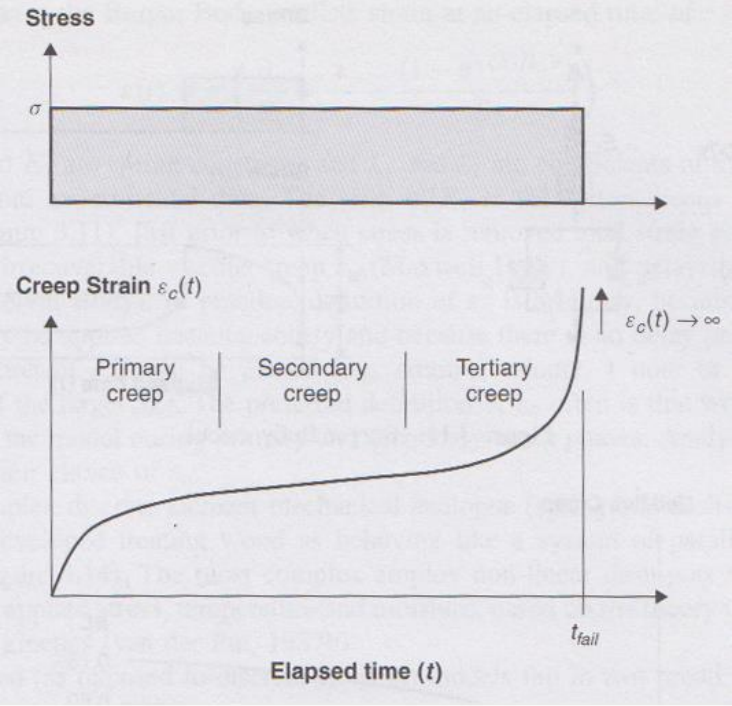

Figure 2. 13: Deformation phases in creep tests (Smith et al. 2003).

All specimens shown in Figure 2.12 are clearly behaving in the secondary creep stage. The duration of primary creep is proportional to the level of sustained load (as reflected by the strain magnitude). The single OT specimen (5E*) may have been entering the tertiary creep stage. This final observation is supported by the fact that this specimen also exhibited a lower residual strength (see Section 2.2.6) indicating the likelihood of some material damage resulting from the high level of sustained loading ($0.8P_{ult}$) in this case.

2.2.4 Creep Recovery

Following creep loading, the bamboo specimens were unloaded and allowed a recovery period of ten days. Depending on specimen orientation and the ratio of ultimate load applied, the average recovery was 83% of the final strain experienced by a given sample. Residual creep strain is

shown in Figure 2.12. The difference between the peak strain under sustained load and the residual strain is the recovered strain. A perfectly elastic system, having 100% recovery would exhibit zero residual strain. The figure shows the recovery of the elastic strain produced by the initial load, but a portion of the plastic strain resulting from the sustained load remained after the loads were removed. These plots mimic the creep recovery plot determined by Burger's Model in Figure 1.3b. Creep recovery ratios are defined as:

$$\left(1-\frac{\varepsilon_{residual}}{\varepsilon_{creep,\max}}\right) \tag{2-6}$$

Creep recovery ratios are given in Table 2.1. The average value of creep recovery for OC specimens was 0.90 while that for OT specimens was 0.81 indicating greater unrecoverable plastic deformation in the OT specimens. Noteworthy values exist in the ratio of strain recovered for specimens 4E and 5E*. These specimens recovered only 68% and 67% of their final strain, respectively, possibly indicating a significant level of plastic deformation in these cases.

An explanation for the different degrees of creep recovery in the OC and OT specimens may be based on the ultimate observed behavior. In the flexural tests to failure, failure always occurs at the tension face of the beam. Because the inner wall of bamboo culm is composed primarily of the lignin matrix, it may be expected to recover more fully than the outer wall which has a higher fiber density. These tension-based failures and compositional differences contribute to the higher recovery of specimens with outer fibers in compression (OC). Furthermore, tension damage to a fiber-reinforced matrix (OT) is associated with components of fiber pull-out and fiber rupture behavior. These components of damage are not recoverable.

2.2.5 Residual Strength

Following 90 days of sustained load and 10 days relaxation under no load, each of the specimens was tested under monotonic bending in order to determine residual (post-creep) strength. The specimens were tested in bending using the same test set-up as the control tests (Fig 2.1) which is also the same loading geometry as the creep tests. Ultimate load, top and bottom MOR (Eqs 2-2 and 2-3) and the maximum deflection are reported in Table 2.1 for all creep and control specimens. Applied load versus deflection and compression and tension strains are shown in Figure 2.14. In these figures, the control specimens are shown plotted from the origin and the post-creep residual strength tests are shifted 30 mm or 40000 με to the right for clarity. It is important to note that the deflection and strain values shown in Figure 2.14 and the deflection values in Table 2.1 for the creep specimens **do not** include the residual deflections and strains. That is, these values are zeroed at the beginning of each flexure test.

The interpretation of residual strength results is intended to determine the effect of creep conditioning on monotonic bending of clear bamboo specimens. Table 2.3 summarizes all calculated modulus of rupture (MOR) values for the eight control tests and sixteen specimens subject to creep testing. MOR is selected as a basis for comparison since this normalizes for dimensional variation (Eqs 2-1 through 2-3). Based on the MOR values shown in Table 2.3, it may be seen that creep had an apparent strengthening effect on the OC specimens. On the other hand, the OT specimens showed a decrease in average (f_r) and top MOR (f_t) values and a small increase in bottom MOR (f_b). This behavior reflects an upward shift of the neutral axis in the creep-tested OT specimens. This apparent behavior reinforces the differences between the cellulose fiber-dense outer regions of the culm wall and the lignin-dominant inner regions. As

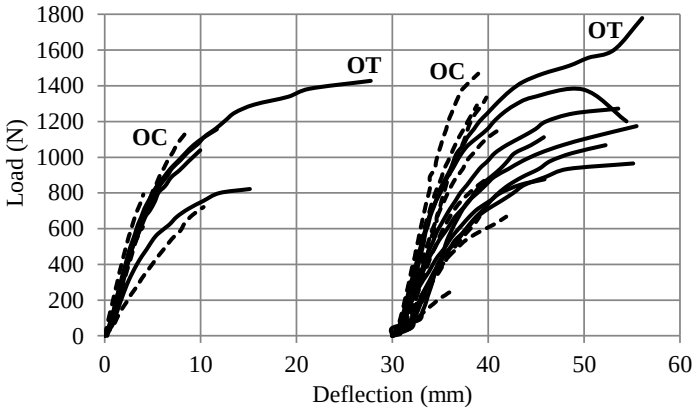

a) load versus midspan deflection

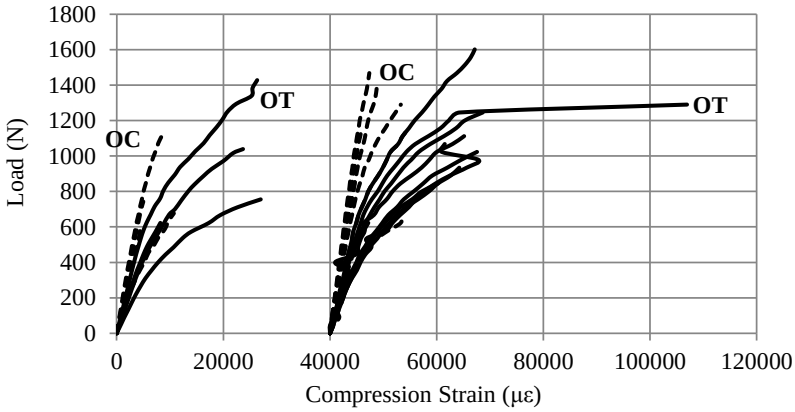

b) load versus compressive strain (shown as positive)

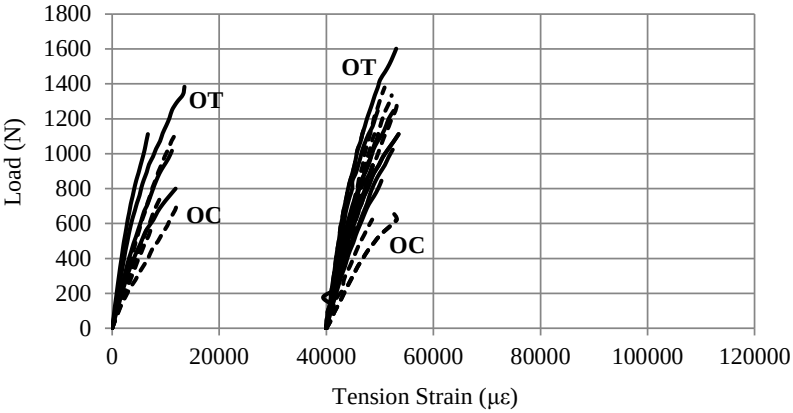

c) load versus tension strain

Figure 2. 14: Residual strength of creep specimens.

described in the previous section in relation to creep recovery, the lignin is quite soft and therefore undergoes little plastic deformation during the creep testing. The fiber-reinforced regions in tension (OT), exhibit a degree of plastic damage possibly associated with fiber rupture and pull-out. Such damage would generally also be reflected in the OT MOR behavior.

The hypothesis that OC and OT behavior represents two distinctly separate data sets was confirmed ($p = 0.0004$) by a applying a t-test to values of f_t and f_b by f_r for each specimen orientation. Because the groups are statistically significant, the theory that the orientation of the specimen essentially develops two different materials is verified.

The level of sustained load applied to the creep specimens had little effect on the residual strengths of the specimen. However, as shown in Figure 2.15, the post-creep MOR of the lignin side of the specimen (f_t for OC and f_b for OT) increased with increased applied creep load. The MOR of the fiber side of the specimen remained essentially constant. Once again, this result indicates that the sustained load has a stiffening effect on the lignin.

Table 2. 3: Modulus of rupture values for control and creep specimens.

Orientation	Control Specimens			Specimens Subject to Creep Loads		
	f_r	f_t	f_b	f_r	f_t	f_b
	(MPa)	(MPa)	(MPa)	(MPa)	(MPa)	(MPa)
OC	71.2	54.9	87.4	89.1	78.4	99.8
OT	101.1	129.8	72.4	94.8	108.4	81.1
all	86.1	92.4	79.9	91.9	93.4	90.4
Standard Deviation (COV)						
OC	12.2 (0.172)	11.7 (0.213)	13.8 (0.158)	20.1 (0.226)	35.3 (0.450)	15.2 (0.152)
OT	23.5 (0.232)	34.4 (0.265)	15.7 (0.217)	7.3 (0.077)	28.6 (0.264)	30.6 (0.378)
all	23.6 (0.274)	46.5 (0.504)	15.9 (0.199)	14.9 (0.162)	34.7 (0.371)	25.3 (0.279)

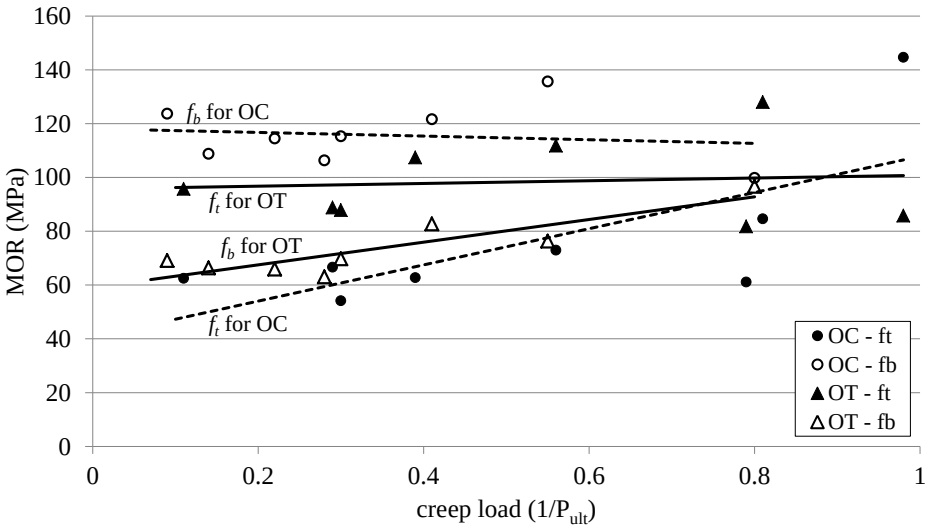

Figure 2. 15: MOR of post-creep specimens versus level of sustained load.

2.3 DERIVED RESULTS AND DISCUSSION OF CREEP TESTS

In addition to the experimentally observed test results discussed in the previous section, there are some useful derived results that are discussed in the context of the experimental data in the following sections.

2.3.1 Neutral Axis Location

By considering compression strain, tension strain and the height dimension, *t*, of each specimen, the neutral axis may be calculated and plotted over time or load, depending on the nature of the applied load (Fig. 2.16). The plots show that the neutral axis shifts toward the outer culm-wall fibers in all cases. This reflects the relative stiffness through the culm wall: the outer fibers are

considerably stiffer and therefore able to carry more load; to maintain equilibrium, this results in the neutral axis shifting toward the stiffer face of the member.

Under creep loads (Figs 2.16a and b) there is very little shift in the neutral axis. Where a shift is identified it is a result of, the compression strain increasing at a slightly greater rate than the tension strain resulting in the neutral axis shifting downward in the specimen section.

The control specimens subject to monotonic load (Figs 2.16c and d) illustrate the same shift toward the outer culm-wall. The neutral axis remains relatively constant through most of the flexure tests indicating an essentially elastic behavior. Small changes in the location of the neutral axis often result from local damage (plasticity, flaws, etc.) and are generally unpredictable in the flexure tests.

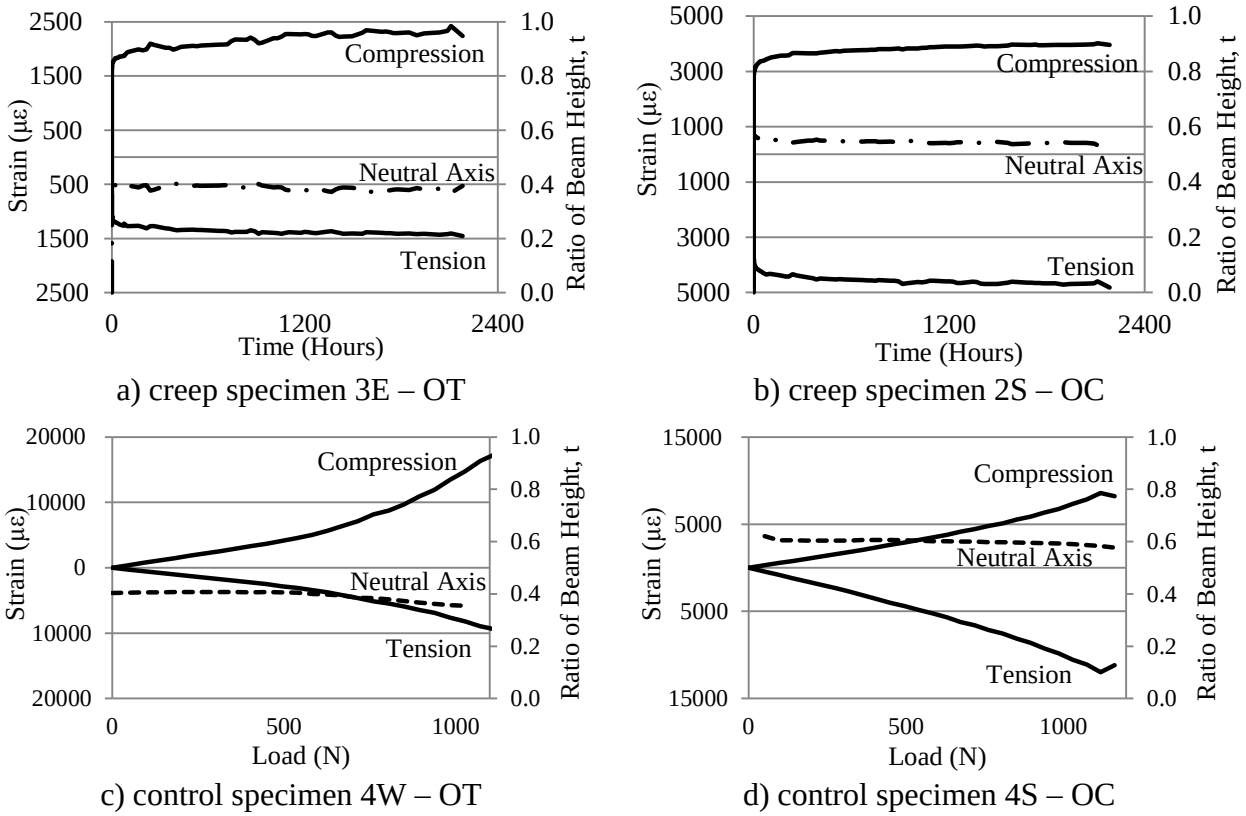

a) creep specimen 3E – OT

b) creep specimen 2S – OC

c) control specimen 4W – OT

d) control specimen 4S – OC

Figure 2. 16: Representative locations of neutral axis for specified load and orientation.

2.3.2 ASTM D6815 Standard Criteria

ASTM D6815-09 *Standard Specification for Evaluation of Duration of Load and Creep Effects of Wood and Wood-Based Products* provides a standard basis for the evaluation of the duration of load and creep on wood and wood-based products subjected to bending stress. These standards were considered in the test configuration used in this study and are applied partially in an effort to evaluate the bamboo tests and to assess whether such standards may be universally adopted for bamboo. Criteria for a successful test include adequate strength over a 90-day period, decreasing creep rate, and limited fractional deflection. Adequate strength over a 90-day period may be confirmed if the 90-day fractional deflection (FD_{90}), defined as the ratio of the deflection at 90 days of sustained loading (D_{90}) to the deflection at one minute after loading (D_1), is less than or equal to 2.0; that is:

$$FD_{90} = \frac{D_{90}}{D_1} \leq 2.0 \tag{2-7}$$

The fractional deflection may be generally defined at any time, t, as D_t/D_1 as shown in Figure 2.17b. The decreasing creep rate may be verified by the inequality:

$$D_{30} - D_1 > D_{60} - D_{30} > D_{90} - D_{60} \tag{2-8}$$

In which the values are deflections at 1 minute and 30, 60 and 90 days as shown in Figure 2.17a. The three terms of Eq. 2-8 represent the creep rates at 30, 60 and 90 days, respectively as shown in Figure 2.17b.

Using Equations 2-7 and 2-8, the performance of each specimen based on the standard criteria of ASTM D6815-09 is evaluated as shown in Table 2.4 which summarizes the 100 day creep history of each specimen. All specimens meet the requirements described for adequate strength after 90 days and limited fractional deflection. The decreasing creep rate is verified in

the majority of specimens; the almost 40% of specimens which do not meet the standard for decreasing creep rate have a creep rate less than 4% of the overall deflection. Because of the nearly constant creep rate after 90 days, the fact that it is not technically decreasing may be attributed to measurement precision although the specimens entering the tertiary stage of creep distortion (Fig. 2.13) cannot be entirely discounted. It is stated in ASTM D6815 that the error in measurement due to both the human operator and the measuring device may be ignored in this case because the scale of the differences in measurements was negligible. It may be assumed, therefore, that at this point the creep rate is relatively constant. In addition to the D6815 standard criteria, the relative creep should also decrease over each 30 day span. This decrease in relative creep is seen in the results (Table 2.4).

The phases of creep development (Fig. 2.13) may be verified by the criteria described. Primary creep is characterized by the fact that the rate of deformation accumulation decreases as time progresses. The majority of specimens meet the decreasing creep rate criteria. Secondary creep corresponds to the phase in which the creep rate is essentially constant in time. This phase is seen in all creep plots (Fig. 2.12) and is evident in the fractional creep and creep rate data (Table 2.4). During the tertiary creep phase, the creep rate increases as time progresses. This is evident in the heavily loaded specimens 5S*, 5E* and 6W*. As described previously (in relation to Fig. 2.11b and 2.12), it was expected that Specimen 5E* certainly entered the tertiary creep stage. Creep rupture occurs after a specimen has experienced the tertiary creep phase to the point of failure (Smith et al. 2003). There is interest in extending the experiment duration under large loads in order to evaluate tertiary creep and eventual creep rupture in a bamboo specimen.

The creep factor is defined as the ratio of the total deflection to the instantaneous deflection. This is the fractional deflection (Eq. 2-7) and is usually desired for ‘long term’

behavior. For timber, this is often described as being ten years' service (see Section 1.3.1). ASTM D6815-09 does not develop a method for determining a creep factor. Instead, the standard institutes a pass-fail system: duration of load in dry conditions must meet the criteria described. Thus, a material passing the standard has a creep factor less than 2.0 which is the value often adopted in design. Thus, the Tre Gai bamboo specimens tested would have generally passed the criteria for creep in timber construction.

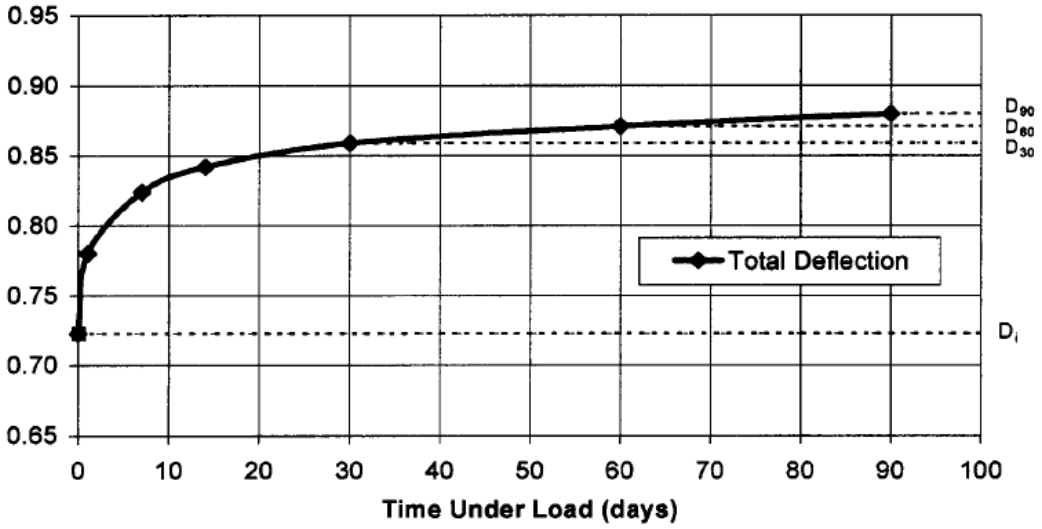

a) total deflection versus time

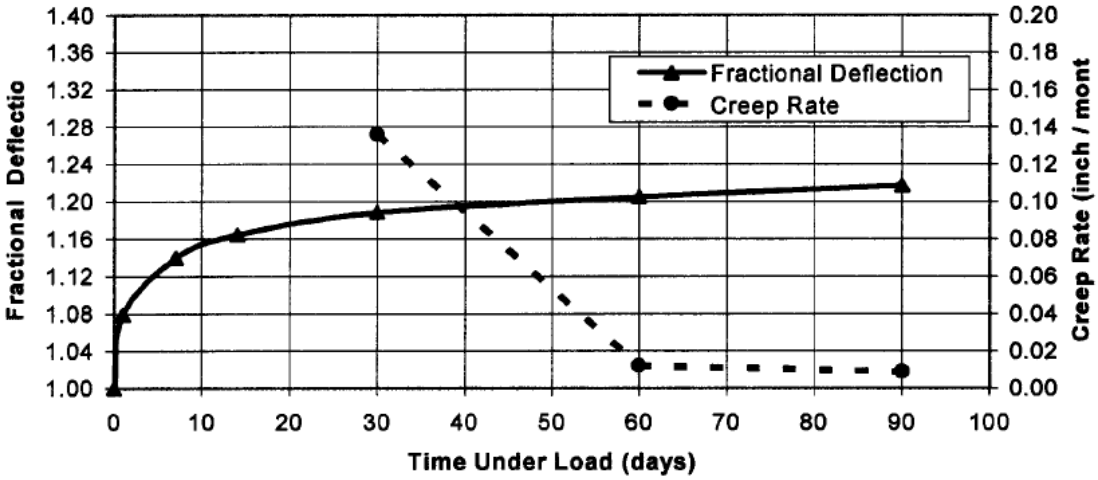

b) fractional deflection and creep rate

Figure 2. 17: Definitions of deflections, creep rate and fractional creep rate (ASTM D6815).

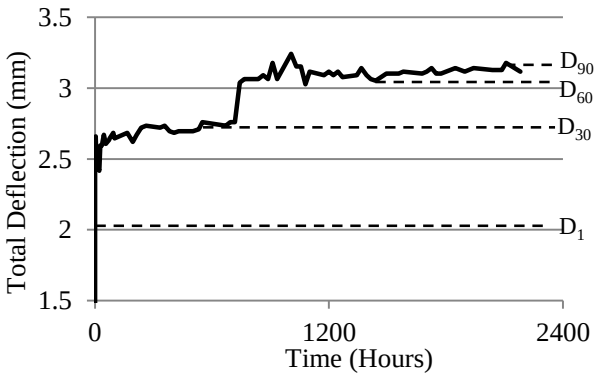

a) deflection versus time 3E – OT

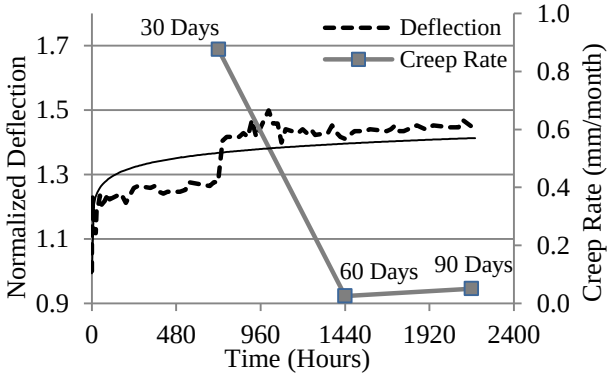

b) fractional deflection and creep rate 3E – OT

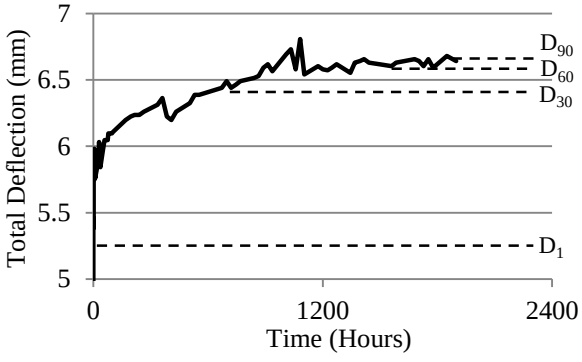

a) deflection versus time 2S – OC

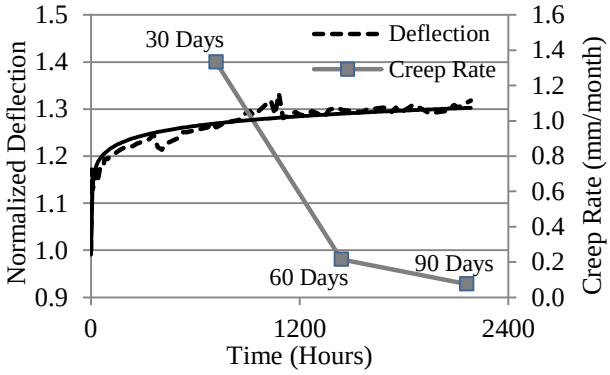

b) fractional deflection and creep rate 2S – OC

Figure 2. 18: Representative deflection plots of creep specimens**.**

Table 2. 4: Summary of creep and total deflections.

Spec.	Ratio of P_{ult}	Orient.	Criteria	Time Under Load (Hours)						
				0.0167 (1 min)	24 (1d)	168 (1 wk)	336 (2 wks)	720 (1 mon.)	1440 (2 mon.)	2160 (3 mon.)
2N	0.44	OC	Total Deflection (mm)	3.21	3.20	3.20	3.10	3.29	3.39	3.39
			Creep Rate (mm/month)					0.08	0.10	0.00
			Fractional Deflection	1.00	1.00	1.00	0.96	1.02	1.06	1.06
2S	0.80	OC	Total Deflection (mm)	5.11	5.88	6.20	6.31	6.44	6.63	6.73
			Creep Rate (mm/month)					1.33	0.19	0.10
			Fractional Deflection	1.00	1.15	1.21	1.24	1.26	1.30	1.32
3N	0.31	OC	Total Deflection (mm)	2.93	3.08	3.22	3.13	3.20	3.35	3.36
			Creep Rate (mm/month)					0.27	0.15	0.01
			Fractional Deflection	1.00	1.05	1.10	1.07	1.09	1.14	1.15
4N	0.57	OC	Total Deflection (mm)	2.28	2.91	2.93	2.95	2.99	2.96	3.08
			Creep Rate (mm/month)					0.41	-0.03	0.11
			Fractional Deflection	1.00	1.13	1.13	1.14	1.16	1.15	1.19
5N	0.29	OC	Total Deflection (mm)	3.18	3.15	3.20	3.18	3.24	3.47	3.57
			Creep Rate (mm/month)					0.06	0.23	0.10
			Fractional Deflection	1.00	0.99	1.01	1.00	1.02	1.09	1.12
5S	0.25	OC	Total Deflection (mm)	2.28	2.64	2.64	2.61	2.64		
			Creep Rate (mm/month)					0.36		
			Fractional Deflection	1.00	1.16	1.16	1.14	1.16		
5S*	1.00	OC	Total Deflection (mm)	4.45	4.73	4.91	4.90	5.00	5.06	5.18
			Creep Rate (mm/month)					2.36	0.06	0.11
			Fractional Deflection	1.95	2.07	2.15	2.15	2.19	2.22	2.27
6N	0.1	OC	Total Deflection (mm)	1.33	1.94	1.82	1.91	1.89		
			Creep Rate (mm/month)					0.56		
			Fractional Deflection	1.00	1.46	1.37	1.44	1.42		
6N*	0.83	OC	Total Deflection (mm)	3.79	3.95	4.42	4.36	4.26	4.28	4.17
			Creep Rate (mm/month)					2.37	0.01	-0.10
			Fractional Deflection	2.85	2.97	3.32	3.28	3.21	3.22	3.14
6S	0.11	OC	Total Deflection (mm)	2.21	2.35	2.24	2.29	2.17	2.23	2.14
			Creep Rate (mm/month)					-0.04	0.06	-0.09
			Fractional Deflection	1.00	1.06	1.02	1.04	0.98	1.01	0.97
2E	0.49	OT	Total Deflection (mm)	3.07	3.24	3.31	3.48	3.48	3.67	3.72
			Creep Rate (mm/month)					0.41	0.19	0.05
			Fractional Deflection	1.00	1.05	1.08	1.13	1.13	1.19	1.21

Table 2. 4 (continued).

Spec.	Ratio of P_{ult}	Orient.	Criteria	Time Under Load (Hours)						
				0.0167 (1 min)	24 (1d)	168 (1 wk)	336 (2 wks)	720 (1 mon.)	1440 (2 mon.)	2160 (3 mon.)
2W	0.31	OT	Total Deflection (mm)	2.52	2.65	2.68	2.52	2.52	2.73	2.71
			Creep Rate (mm/month)					0.00	0.20	-0.01
			Fractional Deflection	1.00	1.05	1.06	1.00	1.00	1.08	1.08
3E	0.33	OT	Total Deflection (mm)	2.16	2.60	2.68	2.72	2.76	3.05	3.12
			Creep Rate (mm/month)					0.60	0.29	0.06
			Fractional Deflection	1.00	1.20	1.24	1.26	1.28	1.41	1.44
4E	0.24	OT	Total Deflection (mm)	2.48	3.06	3.26	3.36	3.48	3.60	3.62
			Creep Rate (mm/month)					1.00	0.11	0.03
			Fractional Deflection	1.00	1.24	1.31	1.35	1.40	1.45	1.46
5E	0.22	OT	Total Deflection (mm)	1.83	2.25	2.35	2.37	2.44		
			Creep Rate (mm/month)					0.61		
			Fractional Deflection	1.00	1.23	1.28	1.30	1.33		
5E*	0.89	OT	Total Deflection (mm)	6.18	7.71	8.29	8.80	9.22	9.58	10.05
			Creep Rate (mm/month)					6.78	0.36	0.47
			Fractional Deflection	3.38	4.22	4.53	4.81	5.04	5.24	5.49
5W	0.16	OT	Total Deflection (mm)	1.58	2.29	2.31	2.33	2.24	2.36	2.41
			Creep Rate (mm/month)					0.66	0.11	0.05
			Fractional Deflection	1.00	1.45	1.46	1.47	1.42	1.49	1.52
6E	0.1	OT	Total Deflection (mm)	1.49	1.71	2.07	2.03	2.12	2.45	2.44
			Creep Rate (mm/month)					0.64	0.33	-0.01
			Fractional Deflection	1.00	1.15	1.39	1.37	1.43	1.65	1.64
6W	0.08	OT	Total Deflection (mm)	1.58	2.15	2.10	2.11	2.13		
			Creep Rate (mm/month)					0.66		
			Fractional Deflection	1.00	1.46	1.42	1.43	1.45		
6W*	0.61	OT	Total Deflection (mm)	3.75	3.96	4.19	4.34	4.33	4.38	4.62
			Creep Rate (mm/month)					2.20	0.05	0.24
			Fractional Deflection	2.54	2.69	2.84	2.95	2.94	2.97	3.14

* values refer to specimens with increased loads

2.4 CONCLUSIONS OF CREEP TESTS

The dearth of information on the creep characteristics of bamboo inspired the development of an experiment focusing primarily on the effect of sustained load on bamboo. A secondary focus was the effect of the orientation of the radial fiber density within the specimens. Contrary to the conclusions of Janssen (1981), who indicated that creep effects in bamboo are negligible (Section 1.3.3), significant creep-induced plastic deformations and strains were observed in the present work.

The orientation of the specimen – whether the fiber-rich outer culm wall is placed in compression or tension (OC or OT, respectively) was found to have significant effect on both the creep behavior and residual strength of creep-conditioned specimens. The results showed that the bamboo loaded with the outer culm-wall in tension (OT) generally exhibited the following when compared to specimens with outer culm-wall in compression (OC).

a) a larger modulus of rupture due to the reinforcing effects of the fibers in tension;
b) a lower apparent modulus of elasticity due to the softer lignin exhibiting high compressive strains; and,
c) a lower residual strength following creep conditioning.

These observations are all explained by the difference in behavior between the fiber-rich outer culm wall and the lignin-rich inner culm wall. Specifically, damage to a fiber-reinforced matrix (OT) in tension exhibits components of fiber pull-out and fiber rupture. These components of damage are not recoverable. The lignin matrix, on the other hand, is soft and behaves in an essentially elastic manner; exhibiting mostly recoverable strains.

As summarized in Figure 2.19, the creep trends based on specimen orientation throughout the loading period are comparable. Although the rates of creep values are similar, the average quantitative relative creep effects are higher in specimens with outer fibers in tension (OT). Similarly, the creep displacement and creep strains are higher in specimens with outer fibers in tension (OT).

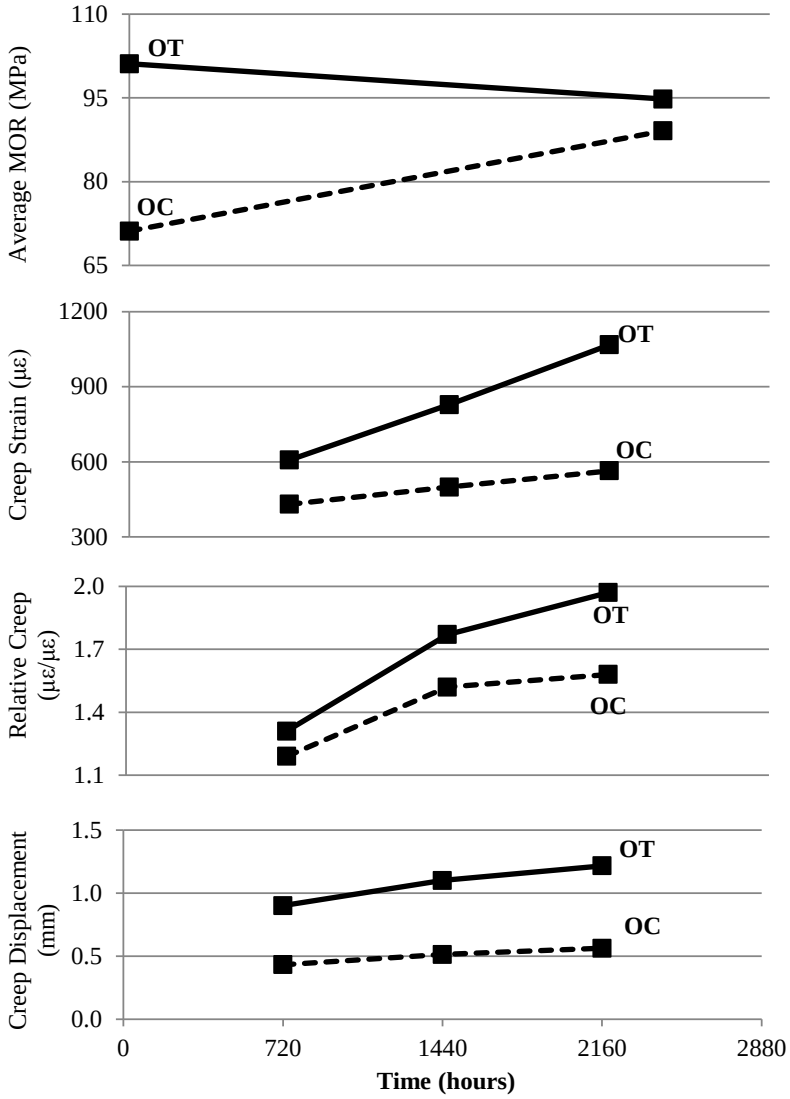

Figure 2. 19: Creep trends within specified orientations.

Additionally when considering residual strength, Figure 2.19 illustrates the strengthening effects of creep on OC specimens and the detrimental effects of creep on OT specimens. The values at zero hours represent the capacity in terms of the average modulus of rupture of control specimens of the specified orientation while the values at 2400 hours represent the residual capacity following 90 days of creep conditioning and subsequent 10 days of recovery. While the average modulus of rupture (f_r) values for control specimens is quite different depending on orientation (f_r = 71.2 MPa for OC and f_r = 101.1 MPa for OT specimens), the average f_r values representing residual capacity are quite similar (f_r = 89.1 MPa for OC and f_r = 94.8 MPa for OT specimens). It is believed that the significant decrease in capacity of OT specimens is related to the damage of the fibers due to creep. Since the orientation of the OC specimens results in a stiffening of the lignin, the creep effects increase the capacity of the bamboo (see section 2.2.6).

The results of the creep experiments showed that the relative creep along with the 90-day strength, creep rate and fractional deflection of bamboo meet or exceed the ASTM 6815 acceptance criteria for wood. The structural similarities between wood and bamboo provide a convenient relationship suggesting that many of the test standards suitable for wood may be applied to bamboo with minor revisions. The Tre Gai bamboo tested met the ASTM 6815 acceptance criteria demonstrating a resistance to extensive creep at high ratios of the ultimate load. This result suggests that for the structural design of bamboo, a load duration factor similar to that of wood may be employed. The load duration factor (Fig. 1.2) may be interpreted as being inversely proportional to the creep factor. Thus the implied creep factor for timber associated with a ten-year sustained load is:

$$\frac{instantaneous\ load\ factor}{ten\ year\ load\ factor} = \frac{2.0}{1.0} = 2.0 \qquad (2\text{-}9)$$

Bamboo is seemingly able to better withstand higher sustained loads than timber; thus the creep factor for permanent loads may be less than 2.0. Table 2.5 provides a comparison of timber design values and average creep ratios determined for Tre Gai bamboo in the present work. The creep factor for bamboo is calculated as:

$$\psi_t = \frac{\varepsilon_0 + \varepsilon_t}{\varepsilon_0} \tag{2-10}$$

Where ψ_t represents the creep factor at a specified time, t, ε_t represents the strain due to creep at time *t* and ε_o represents the initial instantaneous (i.e.: elastic) strain due to the application of the sustained load.

Table 2. 5: Creep factors.

Load Duration	Wood (ANSI, AF&PA NDS 2005)		Tre Gai Bamboo	
	load duration factor, C_D	implied creep factor (Eq. 2-9)	average creep factor (Eq. 2-10)	standard deviation (COV)
Instantaneous	2.00	1.00	1.00	--
10 min.	1.60	1.25	1.04	0.04 (0.04)
7 days	1.25	1.60	1.12	0.19 (0.17)
30 days	--	--	1.14	0.27 (0.24)
60 days	1.15	1.74	1.27	0.18 (0.14)
90 days	--	--	1.29	0.19 (0.15)
10 years	1.00	2.00	--	--
permanent	0.90	2.22	--	--

Clearly additional study is required to extend the creep data to additional species and to an appropriate design life. Nonetheless, based on this initial study, it would appear that bamboo is less susceptible to creep than timber and therefore may warrant design using lower load duration factors. This finding is important in so far as most studies indicate that material resistance factors (so-called φ-factors), when determined for bamboo, will be relatively low

(Mitch 2009 reports a value of $\varphi = 0.44$ in one preliminary study). A lower creep factor for permanent loads may help to mitigate the impact of a low material resistance factor. A final issue that requires resolution is the choice of design life for bamboo; this may be a function of the application, environment and whether the structure is intended to be permanent or temporary.

2.4.1 Future Work

This study of the creep behavior of small clear bamboo specimens has demonstrated an approach for developing creep data for bamboo. Future tests must include a variety of bamboo species since the fiber distribution through the culm wall (for instance) is known to vary from species to species (Grosser and Liese 1971). Additionally, extended-duration tests are required. This is particularly the case for larger sustained loads since some of the present specimens exhibited evidence of entering the tertiary stage of creep behavior indicating that creep failure may have been imminent. The implementation of such a long term project may also facilitate the development of more precise creep coefficients and a better defined series of load duration factors.

Additional experiments which increase the ratio of the ultimate load applied in order to generate creep rupture within the 90-day duration of a standard test may greatly benefit the growing knowledge of creep characteristics in bamboo; particularly the nature of the eventual failure. Finally, progression to larger scale and full-culm specimens is necessary. To observe how a full-culm specimen reacts to a sustained load may help create a relationship between the small-scale and full-scale tests, developing more practical design factors and standardization. Large scale test will provide insight into the interaction of culm-wall fiber densities. In a full-

culm test, the fiber-rich outer culm wall is at both the extreme compression and tension faces of the element. The full-culm creep test must be understood well enough that a relationship to the easier-to-conduct clear specimen tests may be established.

3.0 CULM BENDING TESTS

A total of twelve full-culm bending tests were conducted; each type of test utilized two species with three culms each. Each of the species, *Phyllostachys pubescens* (Moso) and *Bambusa stenostachya* (Tre Gai), were taken from the same batch of bamboo used in Richard's (2013) experiments. For this reason, the results of the experiments may be directly compared.

As described in Section 1.4, motivated by understanding the longitudinal splitting limit state of full-culm bamboo, much work has been conducted on the bending of bamboo culms. Particularly at the University of Pittsburgh, Sharma (2010) and Mitch (2009) evaluated the Mode I transverse tension (splitting) capacity of bamboo. Richard (2013) conducted additional research that studied the interaction between Mode I tension and Mode II shear failures in the mixed-mode conditions that occurs in flexure specimens. The current experiments aim to further evaluate the mixed-mode behavior based on the conclusions that were drawn by Richard. A summary of important conclusions drawn from Richard's work include:

a) Full-culm bending tests (vertical notch mixed-mode failure) exhibit lower strength values than the bowtie (pure Mode II failure), split-pin (pure Mode I failure) and smaller clear bamboo flexural specimens (unnotched mixed-mode failure).
b) Mode II capacity is generally greater than Mode I capacity for brittle, unidirectional fiber-reinforced materials. The mixed-mode failure in the notched culms is dominated by the presence of Mode I stress and the lower Mode I capacity.

c) The tension face notch often affected boundary and loading conditions during the experiment. For these reasons, the location and nature of the notch should be reconsidered.

d) Adjusting the span of the culm and eliminating the notch, allowing for a natural longitudinal shear failure may more accurately capture the interaction between Mode I and Mode II shear failures under four point bending.

This study builds primarily on items c and d and has, as an additional goal, the objective of improving upon the present ISO culm bending tests.

3.1 TEST PROGRAMME

It was determined by Vaessen and Janssen (1997) and later adopted by the ISO (2004b) that a standard span for four point bending of a bamboo culm should have a length that is equal to or greater than thirty times the culm diameter ($S \geq 30D$). Theoretically, a bamboo culm with a length greater than 26D should fail in flexure while one shorter should result in a shear-dominated failure. Because bamboo is particularly susceptible to longitudinal splitting, the series of full-culm bending tests conducted in the present work are intended to capture a mixed-mode shear failure. Three different variations of the standard bamboo culm bending test (ISO 2004b) were conducted in order to obtain the apparent mixed-mode shear capacity of bamboo under flexure loads. A schematic representation of the culm-flexural test is shown in Figure 3.1.

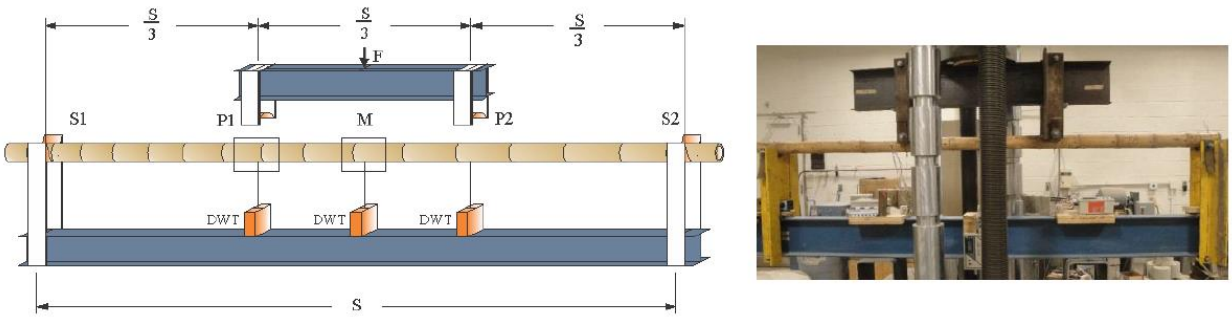

Figure 3. 1: Full-culm bending test arrangement (Richard 2013).

3.1.1 Notched Standard-Span Culm Bending Tests

The first variation on the standard culm bending test implemented in the present study consisted of a full length (S ≥ 30D) culm with symmetric longitudinal notches at midspan (Fig. 3.2). Three Moso specimens were tested in four point flexure over a span of approximately 38D while three Tre Gai culms were tested over spans of 30D. The span and load configurations are shown in Table 3.1. While the culms respected the span requirements for flexure-induced failure, the horizontal notches at midspan were provided to initiate longitudinal splitting and a subsequent failure governed instead by the longitudinal shear capacity of the culm. The notches, located on both sides of the culm at the mid-depth of the culm (Fig. 3.2), were located at the middle of an internode in an effort to capture cracking in both longitudinal directions unaffected by the presence of a node. Aside from these nodal-based restrictions, the notches were located as close to midspan as possible.

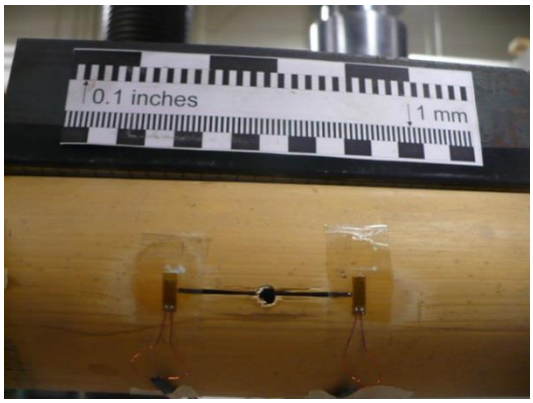

Figure 3. 2: Longitudinal notch and strain gages on standard-span culm.

The notch was achieved by first drilling a 9.5 mm (0.375 in.) hole straight through the culm in order to ensure that the notch was located at the same location on both sides of the culm. A Dremel rotary tool with a stone grinding wheel was then used to produce a notch 25.4mm (1 in.) in length in each longitudinal direction. The total length of the notch was therefore 60.3 mm (2.4 in.). The notch was approximately 3 mm (0.12 in.) wide and passed fully through the thickness of each culm wall. Strain gages were placed at either end of the notch (seen in Fig 3.2) in an effort to capture the strain values at the initiation of cracking.

For testing, draw wire transducers (DWTs) were attached at each support point, at each loading point and at the midspan. The wire, having a nut and bolt configuration connected to its end, was fastened to the culm.

3.1.2 Modified Standard-Span Bending Re-tests

Following initial testing, it was found that, despite the presence of the notches, the long flexible standard-span culms, in three cases, did not exhibit a shear failure prior to exceeding the displacement capacity of the test frame (about 330 mm). In these three cases, the culm was

retested with the notch located in the shear span region of a shorter overall span. As shown in Table 3.1, the notch was located within a 5D shear span while the constant moment region and other shear span were maintained at 8.7D. With this arrangement, it was felt that the shear failure could be 'forced' to occur at the notch in the reduced shear span. Because of space restrictions, the deflections were able to be measured only at the loading and support points for these re-tests.

3.1.3 Short-span Culm Bending Tests

The third variation of the standard-span bending test involved testing over a shorter span, encouraging the culms to experience a 'natural' shear failure. A series of six experiments were conducted with a reduced span. The clear span for the three Tre Gai culms was approximately 15D (Fig 3.3a) while the three Moso culms had spans of about 19D (Fig 3.3b). The short span culms were unnotched, and all tests were run in four point bending with equal third spans (Fig. 3.1).

Strain gages were applied at the four cardinal locations around the culm at midspan as shown in Figure 3.3c. Two of the strain gages were placed perpendicular to the fibers at the culm neutral axis in order to measure tangential strains in the culm. An additional two strain gages were placed parallel to the fibers on the tension and compression faces in order to measure the corresponding flexural strains. Unlike the standard-span culms, only three displacement measurements were able to be recorded for the short span tests. Displacement data was acquired using DWTs located at both supports and at midspan.

3.1.4 Test Configuration and Protocol

The test configuration and protocol duplicate those established for the longitudinal splitting tests performed by Richard (2013); his work may provide additional details concerning the test protocol. Generally, the configuration consisted of 'soft' saddles (designed to accept variation in culm dimension and to not result in any 'hard point' loading that may damage the culm) at loading and support points (Fig. 3.1). Both support and load locations may be moved along their respective steel-beam bases, accommodating the various span lengths required (see Figs 3.1 and 3.3a and b). Span dimensions and test layout of each test is shown in Table 3.1.

The bamboo culms were all loaded in load control at an approximate rate of 4.45 N/sec (1.0 lbs/sec). Along with the load, strains and displacements were recorded. Measurements of the culm geometry (diameter and wall thickness) were recorded upon the completion of the tests; a measurement was taken at the location of failure in addition to the middle of each internode. A summary of measured and calculated geometric properties is provided in Table 3.2.

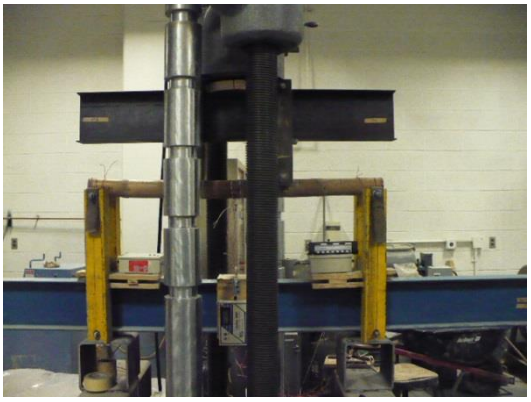

a) Tre Gai specimen (S ≈ 15D)

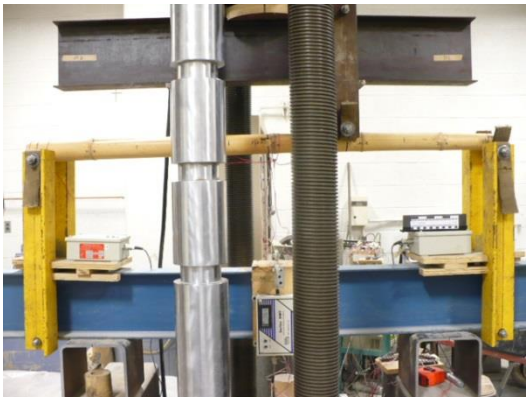

b) Moso specimen (S ≈ 19D)

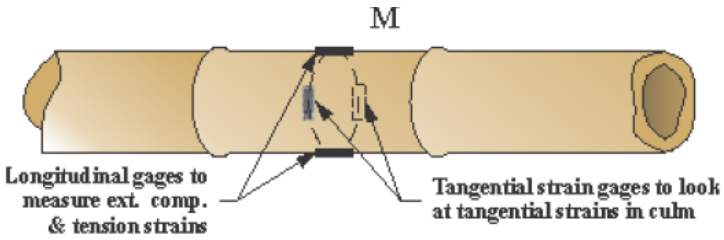

c) longitudinal and tangential strain gages on short span culm (Richard 2013).

Figure 3. 3: Short span culm configuration.

Table 3. 1: Configuration for culm bending tests.

Series	Clear Span		Species	Schematic
	(m)	D = 76.2 mm		
Standard Span	2.90	38D	Moso	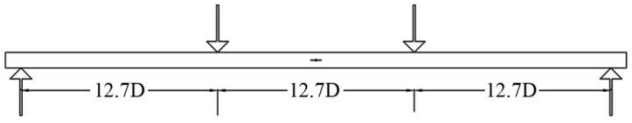
	2.29	30D	Tre Gai	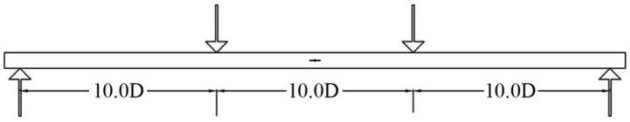
Modified Standard Span Re-test	1.78	22D	Moso	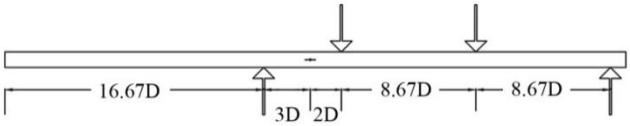
	1.78	22D	Tre Gai	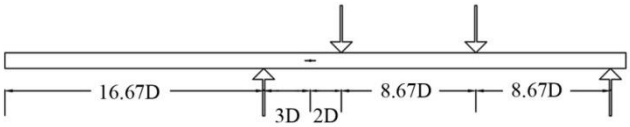
Short Span	1.45	19D	Moso	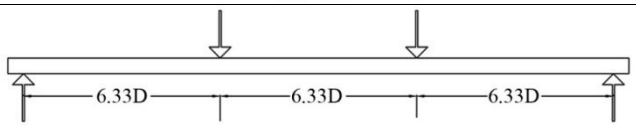
	1.14	15D	Tre Gai	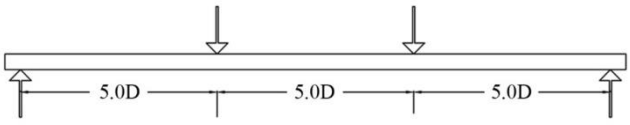

Table 3. 2: Summary of geometric properties and ultimate shear values.

Test		Specimen	Test Span, S		Critical Shear Span	Average Geometric Values at Midspan				Values at Failure				
						Outer Diameter	Wall Thickness	Area	Moment of Inertia	Shear Force	Shear Stress	Avg. Long. Strain	Avg. Tang. Strain	Description of Failure[3]
						D	t	A	I	V	τ	ε_L	ε_T	
			(mm)			(mm)	(mm)	(mm^2)	(mm^4)	(N)	(MPa)	(με)	(με)	
Short Span	1	TG-1B	1143	16.7D	5.6D	68.33	14.7	2477	957456	5761	4.44	8285	415	RTF
	2	TG-9T	1143	16.1D	5.4D	71.16	23.53	3521	1242202	6511	6.43	6400	1500	RTF
	3	TG-9B	1143	16.7D	5.6D	68.34	22.52	3242	1056062	5571	2.99	8765	1465	RTF
	4	M-3T	1448	18.6D	6.2D	77.86	11.12	2331	1334323	5251	4.42	8798	1555	BCF
	5	M-5T	1448	19.9D	6.6D	72.76	7.06	1457	795214	2308	3.14	4140	4233	V@N
	6	M-5B	1448	23.9D	8.0D	60.66	6.09	1045	393703	2595	4.93	8710	1218	V@N
Standard Span	7	TG-5	2286	34.3D	11.4D	66.66	18.75	2822	933517	81243	3.91	-	1118	V@N
	8	TG-10[1]	2286	32.3D	10.8D	70.71	17.7	2948	1151116	> 107350	> 3.99	-	> 771	n.a.
	8R	TG-10R[2]	1778	25.1D	5.6D					5962	8.11	-	1518	V@N
	9	TG-13	2286	29.7D	9.9D	76.97	16.35	3114	1534264	73274	2.72	-	-	V/N
	10	M-6[1]	2896	37.4D	12.5D	77.52	6.59	1469	931967	> 63027	> 4.77	-	> 1500	n.a.
	10R	M-6R[2]	1778	22.9D	5.1D					5956	11.50	-	2621	V@N
	11	M-7[1]	2896	44.2D	14.7D	65.53	7.17	1314	567771	> 69556	> 5.08	-	> 1430	n.a.
	11R	M-7R[2]	1778	27.1D	6.1D					5290	12.23	-	5197	V@N
	12	M-10	2896	44.4D	14.8D	65.24	7.26	1322	564298	131063	9.77	-	11762	V@N

[1] initial test at standard length; maximum shear and strain values observed during test are reported (>) although no failures were observed

[2] retest at shorter shear span

[3] failure modes:

n.a. = no failure observed
BCF = buckling at compression face
RTF = node-induced rupture at tension face
V@N = shear at neutral axis at midspan (i.e.: notch location for standard span specimens)
V/N = shear away from neutral axis at midspan (i.e.: notch location for standard span specimens)

3.2 CULM BENDING TESTS RESULTS

The qualitative and quantitative results for each type of culm test are presented. Correlations between species and tests may be made. The results provide values for ultimate shear stress and ultimate strain for each species and method of testing.

3.2.1 Standard Span Tests Having Notches in Constant Moment Region

The testing of standard span (L > 30D) notched specimens allowed for the acquisition of the longitudinal shear capacity of the Moso and Tre Gai species. Specifically, the ability for the specimen to resist the internal force couple required to resist bending in the constant moment region. The specimens that failed in the original full-span configuration are TG5, TG13 and M10 and are distinguished in Figure 3.4. The equation for longitudinal shear stress in the constant moment region for a culm subject to four point bending is derived from the shear that must be developed to resist the moment couple:

$$\tau = \frac{(M / dv)}{(2t)\left(\frac{S}{3}\right)} = \frac{V}{(2t)\left(\frac{S}{3}\right)} \tag{3-1}$$

Where t represents the average thickness of the culm wall at midspan, S represents the clear span from support to support (i.e.: S/3 is the constant moment regions), M is the value of the moment in the constant moment region, dv is the lever arm of the internal force couple defined as the distance between the centroids of the compression and tension resisting fibers in the cross

section. An approximation of dv is the distance between the centroids of the top and bottom halves of the culm.

The maximum shear stress carried by the Moso specimen in the original configuration (M10) was 9.77 MPa. The average maximum shear stress of Tre Gai specimens in the original configuration was 3.32 MPa (COV = 0.84). This result suggests a difference in behavior between thick (Tre Gai) and thin (Moso) walled species. The sample size is limited due to deflection restrictions of the test configuration; additional tests to be performed on standard span culms with longitudinal notches are required in order to obtain more substantial values.

3.2.2 Re-tests of Standard Span Tests Having Notches in Shear Span

The re-tested specimens had the notch located in a short 5D shear span as shown in Table 3.1. In this configuration, the shear stress is found as:

$$\tau = \frac{VQ}{I(2t)} \tag{3-2}$$

Where V represents shear force, Q represents the first moment of area of the half-culm section above the notch, I is the moment of inertia section and t is the average thickness of the culm wall at the culm cross section being evaluated. As noted in the previous section and shown in Figure 3.4, the Moso species, having a thinner wall than the Tre Gai, exhibit larger shear stresses at failure.

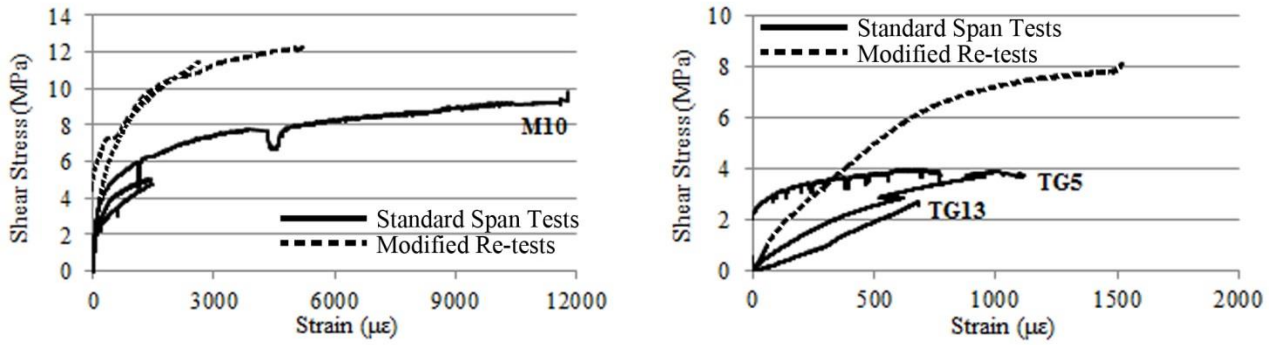

a) Moso specimens b) Tre Gai specimens

Figure 3. 4: Shear stress versus strain in standard span culms.

The average maximum shear stress carried by the Moso specimens in the modified configuration is 11.87 MPa (COV = 0.04). The only Tre Gai specimen that required the modified configuration (TG10) exhibited a maximum shear capacity of 8.11 MPa. Again, due to the inadequate sample size, further testing is required. Such testing should focus on the performance of thick and thin walled sections.

3.2.3 General Notched Specimen Behavior

The majority of specimens with notches (both original and modified configurations) experienced failure at one or both notches (Fig. 3.5). Initial failure at the location of the notch allowed for the collection of important strain values. The recorded average tangential strain values at the instant of crack propagation from the notch for Moso specimens was 6527 microstrain (COV = 0.72). The Tre Gai specimens that failed at the notch location exhibited an average tangential strain value of 1318 microstrain (COV = 0.21). This difference clearly reflects the apparently 'less ductile' behavior of the thick-walled Tre Gai evident in the response shown in Figure 3.5.

Figure 3.6 also illustrates two distinct failure modes exhibited by the species. In the Moso (Fig. 3.6a), the flexible (thin-walled) culm remains relatively intact as the longitudinal failure is characterized by sliding along the failure interface. In the stiffer Tre Gai, the longitudinal failure results in more 'brooming' of the bamboo fibers and separation of the culm halves. This behavior, like similar behavior seen in FRP materials, is hypothesized to be a function of the fiber bundle dimensions.

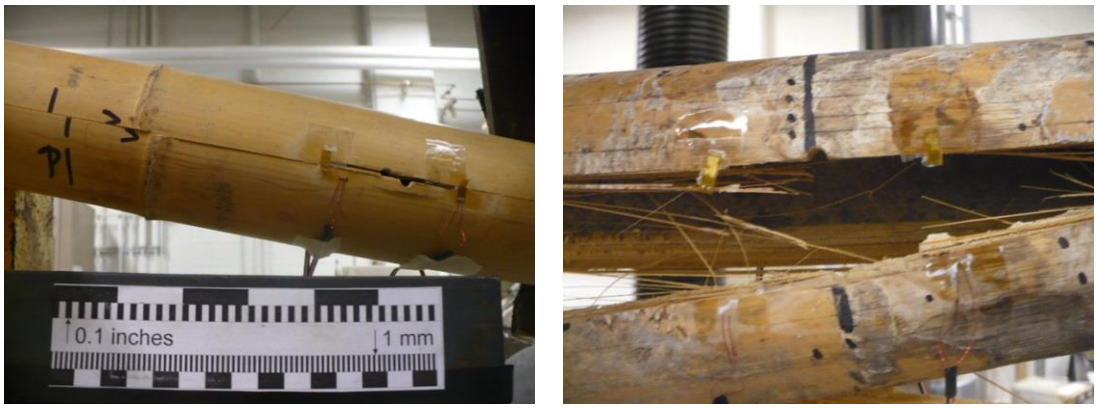

a) Moso specimen M6 b) Tre Gai specimen TG5

Figure 3. 5: Examples of failure at location of notch.

3.2.4 Short Span Bending Tests

Shear stress (determined using Equation 3-2) versus longitudinal flexure-induced strain and tangential shear strain (see Fig. 3.3c for strain gage layout) are shown in Figure 3.6. The shear capacity for Moso and Tre Gai short span culms was 7.24 MPa (COV = 0.59) and 5.49 MPa (COV = 0.41), respectively. In Figure 3.6, the Moso specimens are represented with solid black lines and Tre Gai specimens with solid grey lines. In this short-span test, little variation between

species is observed. The average longitudinal and tangential strain capacities in Moso specimens were 7817 microstrain (COV = 0.16) and 1127 microstrain (COV = 0.55), respectively. For Tre Gai culms, these values were 7216 microstrain (COV = 0.37) and 2335 microstrain (COV = 0.71). In these tests, the majority of the failures initiated at either the tension face or compression face of the culm (see Table 3.2 and Section 3.3.1). Two Moso specimens exhibited longitudinal splitting initiating near the culm neutral axis.

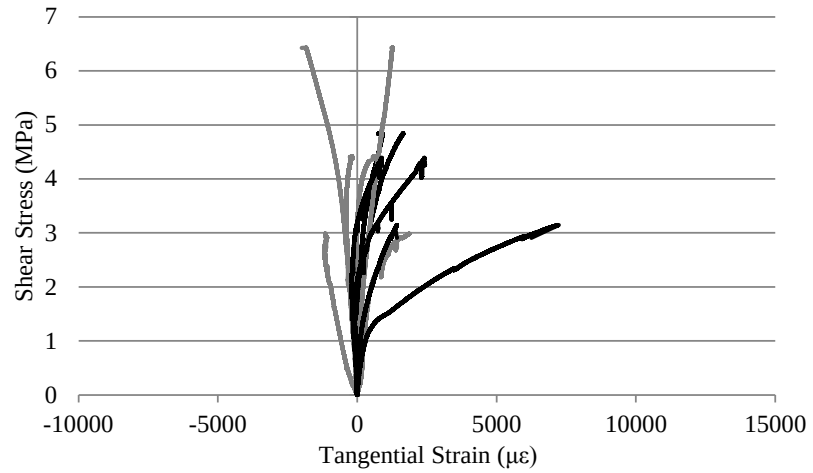

a) tangential strain

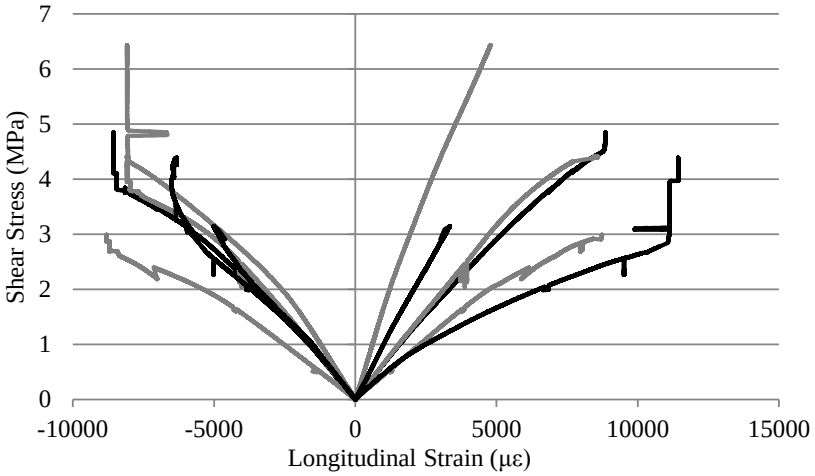

b) longitudinal strain

Figure 3. 6: Shear stress versus strain in short culm tests.

3.3 DISCUSSION OF CULM BENDING TESTS

One objective of the series of culm bending tests was the investigation of the relationship between Mode I tension and Mode II shear failures. A summary of the observed shear stress values at failure is given in Table 3.3, allowing for direct comparisons to be made between modes of failure. The deterioration of the Mode II capacity in bending due to the existence of the Mode I component is illustrated in the values normalized to the bowtie tests which capture only Mode II behavior. The reduced shear span introduces a greater Mode I component to the loading. This is reflected in the Moso results in which the normalized standard bending span capacity is 69% of the Mode II capacity and the shorter span capacity falls to 51%. The Tre Gai tests appear to reflect the opposite trend although, as described below, these culms are believed to have their flexural capacities affected by damage in the nodal regions. The Mode I component clearly affects the bamboo culms under flexure; the pure Mode I (split pin) values are considerably lower (by a factor of about 5) than the Mode II as described in Richard (2013).

Based on these very preliminary findings and considering the simplicity and repeatability of the bowtie test, this test may be best suited for establishing design values for bamboo culms. Longitudinal splitting capacity may be based on a factoring of the Mode II shear obtained from a bowtie tests. To account for the degree of mode mixity, such a factor is affected by the shear span of the culm in bending. Significant additional work is required to establish such a factor which will also, perhaps, be affected by culm geometry (thin or thick-walled) and species.

Table 3. 3: Ultimate shear capacities based on mode of failure.

Species	Bowtie[1]	Short Span	Standard Span Longitudinal Notch	Split Pin[1]
	Mode II	mixed-mode	mixed-mode	Mode I
	τ, MPa (COV)	τ, MPa (COV)	τ, MPa (COV)	$\sigma_{\perp}$, MPa (COV)
Moso	14.20 (0.10)	7.24 (0.59)	9.77 (--)	2.40 (0.24)
Tre Gai	8.65 (0.08)	5.49 (0.41)	3.32 (0.25)	1.52 (0.16)
Normalized Values				
Moso	1.00	0.51	0.69	0.17
Tre Gai	1.00	0.63	0.38	0.18

[1] reported by Richard (2013)

3.3.1 Culm Failure Modes in Bending

Aside from the interest in mixed-mode failure, the experiments also revealed trends in locations and characteristics of failures. The specimen-specific qualitative descriptions of each failure is summarized in Table 3.2. The majority (5/6) of notched culms, both in the original and modified configurations, experienced initial failure at one or both notches; thus longitudinal shear was the governing mode of failure. All three Tre Gai specimens tested in the short span configuration exhibited tension failures which is initially counter-intuitive. Certainly, the increased amount of shrinkage and drying cracks associated with the thick culm walls affected the failure characteristics in the Tre Gai specimens. Additionally, many of the nodes, which are often weaker than the internode to begin with (see section 1.1), also exhibited damage caused by the removal of branches during harvesting. Many of the observed failures were visually traced to these inherent flaws, and the ultimate failure always occurred at the location of a node. These weak nodal areas allowed crack propagation to occur, beginning at the tension face and

continuing towards the neutral axis until failure (Fig 3.7). Finally, the stiff nature of the thick-walled species being subject to relatively large deflections over short spans is expected to affect this behavior.

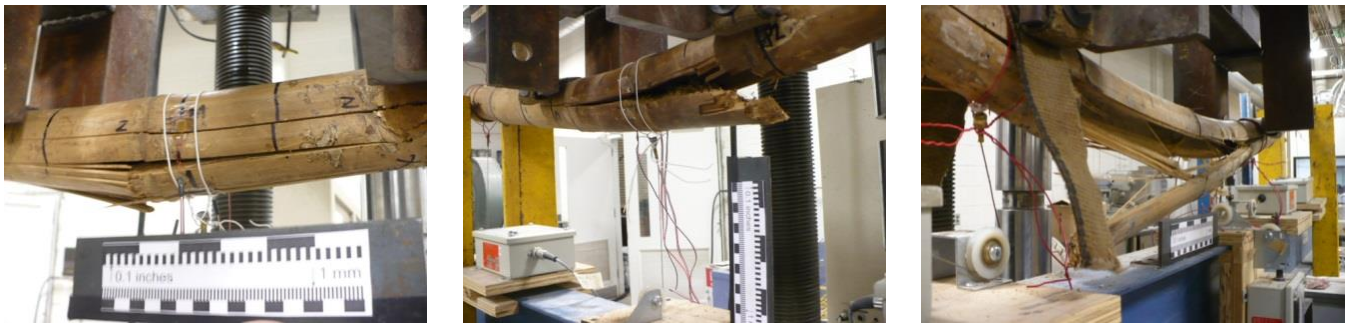

a) culm TG-9B b) culm TG-9T c) culm TG-5

Figure 3. 7: Observed tension failure modes of Tre Gai culms.

The thin-walled Moso specimen that experienced compression failure buckled at midspan (Fig. 3.8a) while the thick-walled Tre Gai compression failure experienced crushing (analogous to a 'crippling' failure) at the loading saddle (Fig. 3.8b). These behaviors are clearly a function of the culm wall thickness, relative to the diameter (i.e.: section slenderness). This is a geometric parameter not previously addressed in the literature.

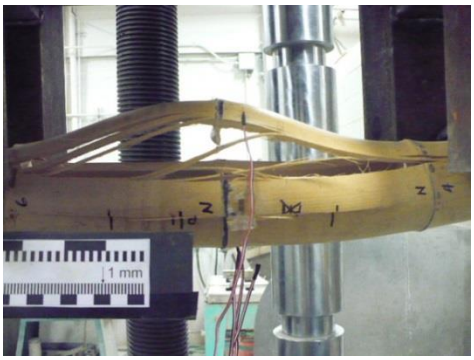

a) Moso culm M3-T

b) Tre Gai culm TG-13 (initial test)

Figure 3. 8: Observed compression failure modes.

Mixed-mode shear failures occurred more often in the thin-walled Moso specimens. As seen in Figure 3.9, such failures are characterized by a noticeable ‘slip’ between the tension and compression regions of the culm subject to bending. The failure occurred at the neutral axis, initiating near midspan and often extended the entire length of the culm (Fig. 3.9a).

a) culm M5-T

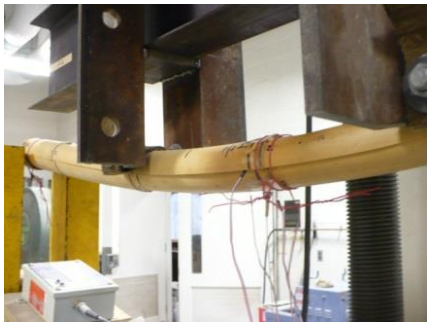

b) culm M5-B

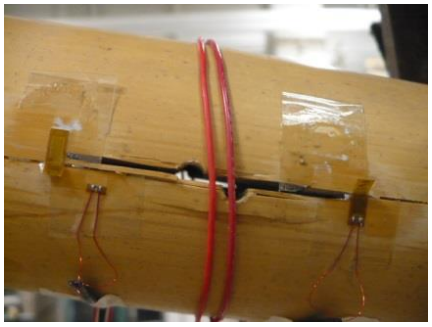

c) culm M6 (retest)

Figure 3. 9: Observed shear failures of Moso culms.

In some tests, failure initiated at only one side of the culm. This resulted in the culm rotating in the test frame affecting the ultimate observed failure. Typically, in this case, the eventual longitudinal failures were not opposite each other on the culm. This behavior should be expected and may be attributed to material variation. Nonetheless, it does highlight the need to capture the initial failure rather than a residual capacity when reporting culm capacities.

3.4 CONCLUSION OF CULM BENDING TESTS

Although further research is required in order to develop standardized criteria in relation to the mixed-mode shear failure in bamboo culms, the current experiments allowed for the development of trends in terms of capacity and characteristics of failures.

Notched standard span (S ≥ 30D) and unnotched short span (S ≥ 15D) full-culm bamboo specimens have provided the opportunity for a quantitative analysis regarding the characteristics of mixed-mode shear failure in bamboo culms under four point bending. The data shows a reduction in the pure Mode II capacity of culms due to the presence of Mode I component.

An overall average longitudinal strain value at crack propagation is given as 7516 microstrain based on all useful data obtained from the unnotched short span tests. The value for overall average tangential strain is 3219 microstrain. The tangential strain value is obtained from both unnotched short span and notched standard span culms. The tangential strain capacity increases slightly (3952 microstrain) when considering only the specimens that failed at their neutral axis location where the tangential strain gages were placed. This value may be more indicative of true tangential strain capacity since it captures ultimate values only, removing lower bound values from the average. Similarly, the ultimate shear stress values obtained from the standard span tests (overall average of 5.47 MPa, COV = 0.69) were quite similar to the same values obtained in the short span tests (overall average of 6.47 MPa, COV = 0.53). This suggests that there may be the opportunity to develop design standards based on shear capacities of culms.

It has previously been suggested that tangential strain capacity is relatively universal among all bamboo species (Arce-Villalobos 1993) and equal to approximately 1200 microstrain. The reasoning for this is that the lignin matrix is relatively unchanged from species to species. The average tangential strain capacity for the current tests, however, is 3219 microstrain. Specifically, the original and modified standard span tests with longitudinal notches yielded an average tangential strain of 4255 microstrain (COV = 1.19); the values for the standard span tests were considerably higher, especially for the Moso culms. The short span shear tests without longitudinal notches, on the other hand, exhibited tangential strain capacities averaging 1731 microstrain (COV = 0.70).

Arce-Villalobos' tests were conducted using small clear specimens placed in tension (parallel to the fibers) having a well-defined (and small) shear plane; so-called S-shaped shear specimens. Comparing *in situ* shear capacity and that derived from small clear specimens is clearly inappropriate. Although, design values obtained from small clear specimens appear to be very conservative, values obtained from full culm bending tests are clearly affected by the degree of mode mixity present. Further study is necessary which must focus on the degree of mixed mode behavior.

Although the inevitable issues of inherent flaws and geometric variability still exist, the experiments have provided a basis of knowledge on a quantitative relationship between Mode II capacity and mixed-mode capacity in bamboo culms under four point bending. Because longitudinal splitting is often considered the dominant mode of failure in bamboo, the ability to develop design values is critical to the structural standardization of the material.

4.0 CONCLUSIONS

The opportunity for bamboo to be utilized as an alternative building material has inspired research towards the standardization of its mechanical properties. The current tests attempted to achieve experimental knowledge on the effect of four point bending on bamboo specimens. The research focuses on: a) creep due to a sustained load; b) longitudinal shear failure under four point bending.

4.1 CREEP TEST CONCLUSIONS

The dearth of information on the creep characteristics of bamboo inspired the development of an experiment focusing primarily on the effect of sustained load on bamboo. A secondary focus was the effect of the orientation of the radial fiber density within the specimens. Small clear flexural specimens were cut radially from the same Tre Gai culm. These were tested in orientations such that either the outer culm wall was in tension (OT) or compression (OC). Control specimens were tested to establish baseline data. Sixteen specimens were subject to sustained loads at different levels for 90 days. Following this creep conditioning, the specimens were left unloaded

for ten days and finally tested to failure so that a comparison may be made with the control specimens.

Contrary to the conclusions of Janssen (1981), who indicated that creep effects in bamboo are negligible, significant creep-induced plastic deformations and strains were observed in the present work. The orientation of the specimen – whether the fiber-rich outer culm wall is placed in compression or tension (OC or OT, respectively) was found to have a significant effect on both the creep behavior and residual strength of creep-conditioned specimens. The results showed that the bamboo loaded with the outer culm-wall in tension (OT) generally exhibited the following when compared to specimens with outer culm-wall in compression (OC).

a) a larger modulus of rupture due to the reinforcing effects of the fibers in tension;
b) a lower apparent modulus of elasticity due to the softer lignin exhibiting high compressive strains; and,
c) a lower residual strength following creep conditioning.

These observations are all explained by the difference in behavior between the fiber-rich outer culm wall and the lignin-rich inner culm wall. Specifically, damage to a fiber-reinforced matrix (OT) in tension exhibits components of fiber pull-out and fiber rupture. These components of damage are not recoverable. The lignin matrix, on the other hand, is soft and behaves in an essentially elastic manner; exhibiting mostly recoverable strains.

As summarized in Figure 2.19, the creep trends based on specimen orientation throughout the loading period are comparable. Although the rates of creep values are similar, the average quantitative relative creep effects are higher in specimens with outer fibers in compression (OC). Conversely, the creep displacement and creep strains are higher in specimens with outer fibers in tension (OT).

Additionally the effects of creep conditioning appears to have a strengthening effect on the residual capacity of OC specimens and a detrimental effects on OT specimens. It is believed that the significant decrease in capacity of OT specimens is related to the damage of the fibers due to creep. Since the orientation of the OC specimens results in a stiffening of the lignin, the creep effects increase the capacity of the bamboo (see section 2.2.6).

The results of the creep experiments showed that the relative creep along with the 90-day strength, creep rate and fractional deflection of bamboo meet or exceed the ASTM 6815 acceptance criteria for wood. This result suggests that for the structural design of bamboo, a load duration factor similar to that of wood may be employed. The load duration factor may be interpreted as being inversely proportional to the creep factor. The 90-day creep factor obtained for Tre Gai bamboo in this study was 1.29 (COV = 0.15). A comparable value for wood falls between 1.75 and 2.00. Clearly additional study is required to extend the creep data to additional species and to an appropriate design life. Nonetheless, based on this initial study, it would appear that bamboo is less susceptible to creep than timber and therefore may warrant design using lower load duration factors. This finding is important in so far as most studies indicate that material resistance factors (so-called φ-factors), when determined for bamboo, will be relatively low. A lower creep factor for permanent loads may help to mitigate the impact of a low material resistance factor. A final issue that requires resolution is the choice of design life for bamboo; this may be a function of the application, environment and whether the structure is intended to be permanent or temporary.

The structural similarities between wood and bamboo provide a convenient relationship suggesting that many of the test standards suitable for wood may be applied to bamboo with minor revisions. Based on the performance of the clear bamboo specimens tested under creep

loads, modification to ASTM D6815 *Standard Specification for Evaluation of Duration of Load and Creep Effects of Wood and Wood-Based Products*, relevant to bamboo are proposed (Table 4.1).

4.1.1 Bamboo Creep: Future Work

This study of the creep behavior of small clear bamboo specimens has demonstrated an approach for developing creep data for bamboo. Future tests must include a variety of bamboo species since the fiber distribution through the culm wall (for instance) is known to vary from species to species (Grosser and Liese 1971). Additionally, extended-duration tests are required. This is particularly the case for larger sustained loads since some of the present specimens exhibited evidence of entering the tertiary stage of creep behavior indicating that creep failure may have been imminent. The implementation of such a long term project may also facilitate the development of more precise creep coefficients and a better defined series of load duration factors.

Additional experiments which increase the ratio of the ultimate load applied in order to generate creep rupture within the 90-day duration of a standard test may greatly benefit the growing knowledge of creep characteristics in bamboo; particularly the nature of the eventual failure. Finally, progression to larger scale and full-culm specimens is necessary. To observe how a full-culm specimen reacts to a sustained load may help create a relationship between the small-scale and full-scale tests, developing more practical design factors and standardization. Large scale test will provide insight into the interaction of culm-wall fiber densities. In a full-culm test, the fiber-rich outer culm wall is at both the extreme compression and tension faces of

the element. The full-culm creep test must be understood well enough that a relationship to the easier-to-conduct clear specimen tests may be established.

Table 4. 1: Suggested amendments to ASTM D6815.

Current ASTM Standard		**Proposed Revisions to Application in Bamboo Creep Tests**
Title	**Content Summary**	
5.1.1 Test Population Requirements	Test population should be representative of the product; short term bending control tests (with identical dimensions to long term specimens) must be conducted; additional tests must be sampled from the initial test population	Current standards must be met; additionally, the specimens must be cut in the radial direction and consist of 50% OT specimens and 50% OC specimens; the variation in wall thickness must be maintained, and the resulting variation in dimensions must be properly compensated. Calculating modulus of rupture, rather than considering specimen capacity is an appropriate method of normalizing specimen geometry.
5.1.2 Specimen Support Conditions	Each test specimen shall be simply supported and loaded by two equal concentrated forces; the span of the specimens shall be split into equal third spans; application of load is in the orientation the product's intended use	Support and loading conditions from current ASTM standard shall remain; however, loads shall be applied in both orientations as stated in 5.1.1 revisions
5.1.3 Moisture Content	Moisture content shall be measured on the short-term specimens immediately after testing and long-term specimens at the completion of the intended load duration (in accordance with ASTM D4442); average moisture content of long term specimens must be within 2% of the average moisture content of short-term specimens	Moisture content shall be measured on the short-term specimens immediately after testing; the long-term test programme should provide a traveller specimen to be stored in the same environment as the creep specimens; moisture content readings shall be taken from this specimen at the start of the experiment, every 30 days and at the conclusion of the experiment. It is recommended that the traveller specimen will also be equipped with strain gages to record the effects of daily changes in moisture content
5.3 Creep Tests	Initial loading rate of creep specimens should not exceed average time to failure of short-span specimens; duration of load should occur for a minimum of 90 days or until creep-rupture; deflection and strain readings should be taken frequently; long term load values are based on a predetermined applied bending stress obtained from short-term tests.	All creep test criteria established by ASTM D6815 should be met; additionally, long-term load values should be determined specific to orientation
5.4 Acceptance Criteria	Test specimens must display a satisfactory performance in the areas of adequate strength (number of failures at 90 days in less than the critical order statistic), decreasing creep rate (change in creep deflection shall progressively decrease from 0-30 days, 30-60 days and 60-90 days) and fractional deflection (the ratio of the deflection after 90 days to the initial deflection should not exceed 2.0)	The concepts of adequate strength, decreasing creep rate and fractional deflection will be applied to long-term bamboo tests; further testing is required in order to develop empirical values for acceptance criteria specific to clear bamboo specimens

4.2 CULM BENDING TEST CONCLUSIONS AND FUTURE WORK

Twelve full-culm bending tests were conducted; each type of test utilized two species (*Phyllostachys pubescens* (Moso) and *Bambusa stenostachya* (Tre Gai)) with three culms each. Notched standard span (S ≥ 30D) and unnotched short span (S ≥ 15D) full-culm bamboo specimens provided the opportunity for a quantitative analysis regarding the characteristics of mixed-mode shear failure in bamboo culms under four point bending. The data shows a reduction in the pure Mode II capacity of culms due to the presence of Mode I component.

The deterioration of the Mode II capacity in bending due to the existence of the Mode I component is illustrated in the values normalized to the bowtie tests which capture only Mode II behavior (Table 3.3). The reduced shear span introduces a greater Mode I component to the loading. This is reflected in the Moso results in which the normalized standard bending span capacity is 69% of the Mode II capacity and the shorter span capacity falls to 51%. The Tre Gai tests appear to reflect the opposite trend although these culms are believed to have their flexural capacities affected by damage in the nodal regions. The Mode I component clearly affects the bamboo culms under flexure; the pure Mode I (split pin) values are considerably lower (by a factor of about 5) than the Mode II. As described in Richard (2013).

Based on these very preliminary findings and considering the simplicity and repeatability of the bowtie test, design values, this test may be best suited for establishing design values for bamboo culms. Longitudinal splitting capacity may be based on a factoring of the Mode II shear obtained from a bowtie tests. To account for the degree of mode mixity, such a factor is affected by the shear span of the culm in bending. Significantly, observed behavior and data are also

clearly affected the culm wall thickness relative to the diameter (i.e.: section slenderness). This is a geometric parameter not previously addressed in the literature.

Although the inevitable issues of inherent flaws and geometric variability still exist, the experiments have provided a basis of knowledge on a quantitative relationship between Mode II capacity and mixed-mode capacity in bamboo culms under four point bending. Because longitudinal splitting is often considered the dominant mode of failure in bamboo, the ability to develop design values is critical to the eventual structural standardization of the material.

Due to the inherent nature of full-culm bamboo, the ability to standardize bamboo as an alternative building material requires extensive investigation and collaboration among researchers. The many advantages associated with the standardization of bamboo create an indisputable incentive. Bamboo is a naturally existing, functionally graded composite-like material with significant mechanical properties which is rapidly renewable and requires little energy or waste to process. With the development of engineering acceptance, bamboo has the potential to provide a proficient and sustainable alternative building material.

CITED REFERENCES

ACI. (2006). *ACI 440.1: Guide for the Design and Construction of Structural Concrete Reinforced with FRP Bars*, Detroit, MI: American Concrete Institute.

Ahmad, M. and Kamke, F.A. (2005). "Analysis of Calcutta bamboo for structural composite materials: physical and mechanical properties." *Wood Science and Technology*, 39(6), 448-459.

Arce-Villalobos, O.A. (1993). "Fundamentals of the design of bamboo structures." Master's Thesis, *Eindhoven University of Technology*, Netherlands.

Allen, E. and Iano, J. (2009). *Fundamentals of building construction: materials and methods*, John Wiley and Sons, Inc., Hoboken, NJ.

Andersson, S., Serimaa, R., Paakkari, T., Saranpaa, P., and Pesonen, E. (2003). "Crystallinity of wood and the size of cellulose crystallites in Norway spruce (Picea abies)." *Journal of Wood Science*, 49(6), 531-537.

ASTM International, (2009). *ASTM D6815-09: Standard Specification for Evaluation of Duration of Load and Creep Effect of Wood and Wood-Based Products*, West Conshohocken, PA: ASTM International.

ASTM International, (2009). *ASTM E2714-09: Standard Test Method for Creep-Fatigue Testing*, West Conshohocken, PA: ASTM International.

ANSI, AF&PA NDS (2005). *National Design Specification (NDS) for Wood Construction with Commentary and Supplement: Design Values for Wood Construction,* Washington, DC: American Forest and Paper Association (AF&PA), American Wood Council (AWC).

Gaylord, E., Gaylord, C., and Stallmeyer, J. (1997). *Structural engineering handbook,* McGraw-Hill, New York, NY.

Grosser, D. and Liese, W. (1971). "On the anatomy of Asian bamboos, with special reference to their vascular bundles." *Wood Science and Technology*, 5(4), 290-312.

Harries, K.A., Sharma, B., and Richard, M.J. (2012). "Structural use of full culm bamboo: the path to standardization." *International Journal of Architecture, Engineering and Construction*, 1(2), 66-75.

Hashin, Z. (1983). "Analysis of composite materials – a survey." *Journal of Applied Mechanics*, 50(3), 481-505.

ISO (International Organization for Standardization), (2004a). *International Standard ISO 22156:2004 (E), Bamboo – Structural Design.* Geneva, Switzerland: ISO.

ISO (International Organization for Standardization), (2004b). *International Standard ISO 22157-1:2004 (E), Bamboo – Determination of Physical and Mechanical Properties – Part I: Requirements.* Geneva, Switzerland: ISO.

ISO (International Organization for Standardization), (2004c). *International Standard ISO 22157-2:2004 (E), Bamboo – Determination of Physical and Mechanical Properties – Part II: Laboratory Manual.* Geneva, Switzerland: ISO.

Janssen, J. (1981). “Bamboo in building dtructures”. Doctoral Thesis, *Eindhoven University of Technology,* Netherlands.

Kanzawa, E., Aoyagi, S., and Nakano, T. (2011). “Vascular bundle shape in cross-section and relaxation properties of Moso bamboo (Phyllostachys pubescens).” *Materials Science and Engineering: C,* 31(5), 1050-1054.

Lilholt, H. (1985). “Creep of fibrous composite materials.” *Composites science and Technology,* 22(4), 277-294.

Limaye, V.D. (1952). “Strength of bamboo (Dendrocalamus strictus).” *Indian Forester,* 78(11), 558-575.

Liu, X., Elmahdy, A.E., Wildman, R.D., Ashcroft, I.A., Ruiz, P.D. (2011). “Experimental investigation and material modelling of fresh and UV aged Japanese lacquer (Urushi).” *Progress in Organic Coatings,* 70(4), 160-169.

Low, I.M., Che, Z.Y., and Latella, B.A. (2006), “Mapping the structure, composition and mechanical properties of bamboo.” *Journal of Materials Research,* 21(8), 1969-1976.

Mileiko, S.T. (1971). “Creep and long-term strength of a fibrous composite.” *Strength of Materials,* 3(7), 775-763.

Mitch, D. (2009). “Splitting Capacity Characterization of Bamboo Culms.” University of Pittsburgh Honors College Thesis, *University of Pittsburgh,* Pittsburgh, PA.

Mitch, D. (2010). “Structural behavior of grouted-bar bamboo column bases.” Master’s Thesis, *University of Pittsburgh,* Pittsburgh, PA.

Obataya, E., Kitin, P., and Yamauchi, H. (2007). "Bending characteristics of bamboo (Phyllostachys pubescens) with respect to its fiber-foam composite structure." *Wood Science and Technology*, 41(5), 385-400.

Richard, M.J. (2013). "Assessing the performance of bamboo structural components." Doctoral Dissertation, *University of Pittsburgh*, Pittsburgh, PA.

Riley, W., Sturges, L., and Morris, D. (2002). "Stress-strain-temperature relationships." *Statics and mechanics of materials: an integrated approach,* John Wiley and Sons, Inc., New York, NY, 114-123.

Sekhar, A.C. and Rawat, B.S. (1956). "Strength tests on bamboos." *Indian Forest Leaflet,* 147 (Timber Mechanics), Government of India, New Delhi, India.

Sharma, B. (2010). "Seismic performance of bamboo structures." Doctoral Dissertation, *University of Pittsburgh*, Pittsburgh, PA.

Smith, I., Landis, E., and Gong, M. (2003). *Fracture and Fatigue in Wood*. John Wiley and Sons Ltd., West Sussex, UK.

Vaessen, M.J. and Janssen, J.J.A. (1997). "Analysis of the critical length of culms of bamboo in four-point bending tests." *Heron*, 42(2), 113-124.